The Impact of Liquefaction on the Microstructure of Cohesionless Soils

by

Angel Gutierrez

A Thesis Presented in Partial Fulfillment
of the Requirements for the Degree
Master of Science

Approved July 2013 by the
Graduate Supervisory Committee:

Edward Kavazanjian, Chair
Claudia Zapata
Sandra Houston

ARIZONA STATE UNIVERSITY

August 2013

ABSTRACT

The effect of earthquake-induced liquefaction on the local void ratio distribution of cohesionless soil is evaluated using x-ray computed tomography (CT) and an advanced image processing software package. Intact, relatively undisturbed specimens of cohesionless soil were recovered before and after liquefaction by freezing and coring soil deposits created by pluviation and by sedimentation through water. Pluviated soil deposits were liquefied in the small geotechnical centrifuge at the University of California at Davis shared-use National Science Foundation (NSF)-supported Network for Earthquake Engineering Simulation (NEES) facility. A soil deposit created by sedimentation through water was liquefied on a small shake table in the Arizona State University geotechnical laboratory. Initial centrifuge tests employed Ottawa 20-30 sand but this material proved to be too coarse to liquefy in the centrifuge. Therefore, subsequent centrifuge tests employed Ottawa F60 sand. The shake table test employed Ottawa 20-30 sand. Recovered cores were stabilized by impregnation with optical grade epoxy and sent to the University of Texas at Austin NSF-supported facility at the University of Texas at Austin for high-resolution CT scanning of geologic media. The local void ratio distribution of a CT-scanned core of Ottawa 20-30 sand evaluated using Avizo® Fire, a commercially available advanced program for image analysis, was compared to the local void ratio distribution established on the same core by analysis of optical images to demonstrate that analysis of the CT scans gave similar results to optical methods. CT scans were subsequently conducted on liquefied and not-liquefied specimens of Ottawa 20-30 sand and Ottawa F60 sand. The resolution of F60 specimens was inadequate to establish the local void ratio distribution. Results of the analysis of the

Ottawa 20-30 specimens recovered from the model built for the shake table test showed that liquefaction can substantially influence the variability in local void ratio, increasing the degree of non-homogeneity in the specimen.

DEDICATION

This thesis is dedicated to my parents, Jose Angel and Margarita Gutierrez, who have provided both emotional and financial support in my academic career. Without their guidance and life lessons I would not have been able to reach my goals.

ACKNOWLEDGMENTS

I would like to express my gratitude to my advisor, Dr. Edward Kavazanjian Jr., for giving me the opportunity to be his pupil. His guidance and the knowledge he has passed onto me have been imperative in me reaching my educational goals. In short, thanks Ed, I wouldn't be here if you hadn't given me a chance when I knocked on your office door.

I also want to thank Peter Goguen for teaching me how to use laboratory equipment and helping me design a shake table. He was always on top of things when I needed him.

I would also like to thank all the staff at the UC Davis Center for Geotechnical Modeling. All of them helped me get the necessary testing done in the short time I could be in Davis.

Finally, I would like to thank Elliot Bartell, David Czupak, and Kanyembo Katapa for all their help and hard work. David and Kanyembo paved the way for this research study and Elliot was always there to help out.

TABLE OF CONTENTS

Page

LIST OF TABLES vi

LIST OF FIGURES vii

CHAPTER

1 INTRODUCTION 1

1.1 Objective 1

1.2 Background 2

1.3 Organization of Thesis Work 4

2 BACKGROUND 6

2.1 Introduction 6

2.2 Liquefiable Soil Deposit Preparation 6

2.2.1 ASU Model Container 7

2.2.2 Air-Pluviation 9

2.3 Centrifuge Testing 10

2.4 Acquisition of Undisturbed Samples 13

2.5 Stabilization of Soil Samples 14

2.6 Soil Imaging 17

2.6.1 Bright Field Microscopy Imaging of Stabilized Soil Specimens 17

2.6.2 CT Scan Imaging of Soils 21

2.7 Stress-Strain of Ottawa 20-30 Crystal Silica Sand 22

3 RESEARCH PROGRAM 25
3.1 Introduction 25
3.2 Soils Employed in the Research 26
3.2.1 Ottawa 20-30 26
3.2.2 Ottawa F60 28
3.3 Model Preparation Methods 30
3.3.1 Centrifuge Model Preparation 30
3.3.2 Shake Table Model Preparation 33
3.4 Model Testing 34
3.4.1 Centrifuge Model Testing 34
3.4.2 Shake Table Testing 35
3.5 X-Ray CT Scans 36
3.5.1 CT Scan Image Analysis 37
3.5.2 Importance of Thresholding 41
4 MODEL TESTING 43
4.1 Test Soils 43
4.1.1 Ottawa 20-30 43
4.1.2 Ottawa F60 46
4.2 Centrifuge Testing 48
4.2.1 Initial Ottawa 20-30 Tests 48
4.2.2 Ottawa F60 Tests 49
4.2.3 Instrumentation 52
4.3 Shake Table Testing 53

4.4 Core Specimens 54

5 CT SCANS AND ANALYSIS 57

5.1 Introduction 57

5.2 Comparison of CT Scans and Optical Imaging Results 57

5.3 Impact of Liquefaction on Ottawa 20-30 Sand Specimens 60

5.4 CT Scans for Ottawa F60 Sand Specimens 65

6 SUMMARY AND CONCLUSIONS 66

6.1 Summary 66

6.2 Conclusions 67

6.3 Recommendations for Future Work 68

REFERENCES 69

APPENDIX

A OTTAWA 20-30 SAND PRODUCT FACT SHEET 71

B OTTAWA F60 SAND PRODUCT FACT SHEET 73

LIST OF TABLES

Table Page

2.1 Scale Factors for Centrifuge Model Tests. (Kutter, 1992) 12

2.2 Initial Properties of Undrained Baseline Test Specimens. (Katapa, 2011) 23

3.1 Physical Characteristics of Ottawa 20-30. (Czupak, 2011) 28

3.2 Physical Characteristics of Ottawa F60. 29

4.1 Summary of Ottawa 20-30 Sand Centrifuge Tests 49

4.2 Summary of Ottawa F60 Sand Centrifuge Tests 52

4.3 Instrumentation for UC Davis Centrifuge Tests 53

4.4 Summary of ASU Shake Table Tests (Ottawa 20-30 sand) 54

4.5 Core Specimen Details 55

5.1 Mean Void Ratio for CT and BFM for Different Subvolumes 58

LIST OF FIGURES

Figure Page

2.1 Model Container (box). (Katapa, 2011) 8

2.2 Box Lid. (Katapa, 2011)..... 8

2.3 Pluviation Fall Height-Density Relationship for Ottawa 20-30 Crystal Silica Sand. (Katapa, 2011) 10

2.4 Modified Triaxial Cell Setup. (Czupak, 2011)..... 15

2.5 Specimen Drying Setup. (Czupak, 2011) 16

2.6 Work Flow Diagram for Image Processing. (Czupak, 2011) 19

2.7 Standard Deviation vs. Average Particle Count. (Czupak, 2011)..... 21

2.8 Undrained Stress-Strain Response of Ottawa 20-30 Sand Baseline Specimens. (Katapa, 2011)..... 23

2.9 Undrained Stress-Strain-Strength Results Plotted on Confidence Interval Developed From the Baseline Undrained Triaxial Tests. (Katapa, 2011) 24

3.1 Grain Size Distribution for Ottawa 20-30. (Czupak, 2011)..... 27

3.2 F60 Grain Size Distribution 29

3.3 Mounted Model Ready for Centrifuge Testing 32

3.4 Schaevitz Centrifuge. (UC Davis, 2013) 34

3.5 Shake Table Apparatus 36

3.6 Unprocessed CT Scan Image of a Soil Specimen 38

3.7 Avizo® Fire Procedure 40

3.8 Filtered Subvolume of a Soil Specimen 41

3.9 Low Quality Histogram for Thresholding 42

3.10 Higher Quality Histogram for Thresholding 42

4.1 Ottawa 20-30 Sand Undrained Triaxial Compression Loading Test Results for a Relative Density of 60% at an Isotropic Confining Pressure of 60 kPa 44

4.2 Ottawa 20-30 Sand Drained Triaxial Compression Loading Test Results for a Relative Density of 60% at an Isotropic Confining Pressure of 100 kPa 45

4.3 Ottawa F60 Sand Undrained Triaxial Compression Loading Test Results for a Relative Density of 53% at an Isotropic Confining Pressure of 60 kPa 47

4.4 Failure Plane for Model C3-3 Embankment Test 51

5.1 Local void ratio distribution for (a) 8000 x 8000 microns for BFM (Czupak, 2011) and (b) 4000 x 4000 microns for CT 59

5.2 Standard Deviation vs. Subvolume Size of CT Scan Images 60

5.3 (a) Mean void ratio vs. subvolume size and (b) standard deviation vs. subvolume size for baseline Ottawa 20-30 sand specimen (BO1) 62

5.4 (a) Mean void ratio vs. subvolume size and (b) standard deviation vs. subvolume size for liquefied Ottawa 20-30 sand specimen (S1-1-1) 63

5.5 Frequency Histogram of Local Void Ratio in Liquefied Specimen 65

Chapter 1

1 INTRODUCTION

1.1. Objective

The objective of this study was to evaluate the impact of earthquake-induced liquefaction on the microstructure of cohesionless soils. The key measure of soil microstructure used for this purpose was the distribution of local void ration. To achieve this objective, it was necessary to obtain images of the structure of cohesionless soils before and after liquefaction from which local void ratio could be quantified. This research is part of National Science Foundation (NSF) Project No. CMMI-0936421, "NEESR-CR: Properties of Cohesionless Soil Subsequent to Liquefaction and Resedimentation" (the NSF project). The NSF project is a collaborative effort among Arizona State University (ASU), Stanford University (Stanford), and Bucknell University (Bucknell). The ASU component of the project involved centrifuge and shake table testing to induce liquefaction in cohesionless soil, extraction and stabilization using optical grade epoxy of relatively undisturbed samples before and after liquefaction, and imaging and image analysis of the stabilized soil samples to quantify the local void ratio distribution. Stabilized soil samples were initially imaged using both an optical method (Bright Field Microscopy) and X-ray Computed Tomography (CT). Once the simpler CT imaging method was shown to provide results similar to the optical method, the CT method was employed for the balance of the work. The CT images of the stabilized soil samples before and after liquefaction were analyzed using advanced 3D image

analysis software to establish the local void ratio distribution in the samples. The work also included triaxial compression shear tests to evaluate the shear strength and stress-strain properties of the soil prior to liquefaction and to demonstrate that the sample recovery process produced relatively undisturbed specimens.

1.2 Background

The object the work conducted for this thesis was to investigate the impact of earthquake-induced liquefaction on the microstructure of a granular soil. The primary index of the changes in the soil microstructure due to liquefaction was the local void ratio distribution. Changes in local void ratio distribution were investigated through shake table testing, centrifuge testing, undisturbed sampling, stabilization of recovered specimens, microstructure imaging of the stabilized specimens, and image analysis.

Earthquake-induced liquefaction has been known to cause billions of dollars in structural damage in earthquake prone areas. This damage has led to extensive research in the field of liquefaction and post-liquefaction behavior of soil. However, there is little to no work on the impact of liquefaction on soil structure.

Immediately after liquefaction has occurred, the soil no longer has a well-defined soil structure and behaves like a viscous liquid. As the liquefaction process ends, the soil particles within the viscous liquid settle until a new well-defined soil structure is formed. Since the soil particles did not, in general, follow the same sedimentation process as the original soil structure, the new microstructure of the soil may differ significantly from the pre-liquefaction soil microstructure (Borja et al. 2008). A difference in microstructure can lead to changes in important engineering soil properties like shear strength. In

particular, a change in local void ratio homogeneity can lead to strain localization effects during shear that may radically changes the stress-strain-strength properties of the soil.

Borja et al. (2008) hypothesized that the microstructure of soil resedimented after liquefaction would not be homogenous. For example, the new soil structure could have loose soil pockets and there could be segregation of soil particles and changes in density of the soil between the upper and lower boundaries of the liquefiable soil layer. A non-homogeneous soil structure could lead to a lower shear strength due to strain localization effects.

Previous research conducted at Arizona State University (ASU) has laid down the groundwork for this phase of the NSF project. A container similar to the rigid box employed at the UC Davis Center for Geotechnical Modeling on the Schaevitz centrifuge employed in this research was constructed for the ASU soils laboratory by Katapa (2011). Katapa (2011) also developed a method for pluviating granular soil into the box, saturating granular soil in the box, and recovering undisturbed specimens of granular soil from the box by freezing the soil mass. Frozen soil samples of 1.4" and 2.8" diameter were recovered by coring from the frozen soil mass in order to obtain relatively undisturbed cohesionless soil samples. The results of triaxial compression tests on 2.8" diameter cores were compared to similar tests on specimens formed in a split mold without freezing to demonstrate the effectiveness of the sampling technique. Cores recovered from the frozen 1.4" diameter cores were stabilized using epoxy and subject to optical imaging for microstructural analysis by Czupak (2011). This work builds upon the previous work by using the Katapa (2011) model preparation and sample recovery techniques and the Czupak (2011) stabilization technique to prepare samples of soil

recovered before and after liquefaction for CT scans and image analysis. The Czupak (2011) optical image analysis was also employed as a check on the accuracy of the CT scan image analysis.

1.3 Organization of Thesis Work

This dissertation is divided into six chapters, including this introductory chapter that gives a brief background and overview of the research conducted. Chapter 2 covers previous work related to the creation of liquefiable soil deposits, the acquisition of undisturbed specimens of cohesionless soils, specimen stabilization methods, stabilized specimen imaging techniques, and specimen microstructure quantification. Chapter 3 covers the research plan that was employed to achieve the goals of this part of the NSF project. Chapter 3 includes a description of the experimental methods employed in the research. These methods include microstructural analysis of granular soil specimens, procedures for the centrifuge tests conducted at the University of California at Davis, procedures for the shake table test conducted at ASU, procedures for the recovery, stabilization, and imaging of intact, presumably undisturbed soil specimens, and processing of the images of the recovered soil specimens for microstructure evaluation. Chapter 3 also describes the material properties of the two granular soils employed in the research: Ottawa 20-30 Crystal Silica and Ottawa F60 Crystal Silica sand. The material properties addressed in Chapter 3 include index properties (e.g. grain size, minimum and maximum void ratios, and relative density) and engineering properties (e.g. shear strength) for the baseline (pre-liquefaction) specimens. Chapter 4 describes the UC Davis centrifuge and ASU shake table tests, including the creation of the liquefiable soil

deposit and the recovery and stabilization of specimens. Chapter 5 covers specimen CT scanning and microstructural analysis of the CT scan images. Chapter 6 presents conclusions drawn from comparison of the microstructural properties of specimens before and after liquefaction along with recommendations for future work.

Chapter 2

2 BACKGROUND

2.1 Introduction

The purpose of this study was to characterize the local void ratio distribution of cohesionless soils before and after earthquake-induced liquefaction. Success of the research program required developing techniques for creating reproducible deposits of liquefiable cohesionless soil, simulating earthquake-induced liquefaction within those deposits, recovering intact specimens of saturated cohesionless soil both before and after liquefaction for microstructural imaging, fixing the structure of the recovered specimens to facilitate imaging, and microstructural imaging and image analysis. This chapter identifies the available techniques for accomplishing these objectives, provides the rational for the particular techniques chosen for use in this study, and provides background on the selected techniques.

2.2 Liquefiable Soil Deposit Preparation

Liquefiable soil deposits were created in two model containers: a container constructed specifically for this purpose in the ASU soil laboratory and the rigid box for the small Schaevitz centrifuge at the UC Davis Center for Geotechnical Modeling. However, the ASU box was modeled after the Davis box so that the same soil deposit preparation technique could be used in both boxes. The ASU box was used to develop the soil deposit preparation and sample recovery techniques before mobilizing to the UC Davis facility for centrifuge testing and for creation of soil deposits for subsequent liquefaction on a shake table in the ASU soil laboratory.

2.2.1 ASU Model Container

Katapa (2011) developed a rigid box at ASU that would be compatible with the small Schaevitz centrifuge at UC Davis. To do so, Katapa (2011) used the Schaevitz centrifuge rigid box as the basis for design for the ASU container. Based upon information given by Fiegel et. al (1994), the dimensions of the Schaevitz centrifuge rigid box are 559 mm by 279 mm by 179 mm. The ASU box was fabricated to essentially the same dimensions out of aluminum, with a Lexan front face that allowed for observation of the propagation of the freezing front in the soil prior to sampling and of visual signs of liquefaction in the soil deposit after liquefaction on the ASU shake table. The ASU container has five ports at the bottom to allow for the introduction of water for model saturation. These ports can also work as drainage ports. Katapa (2011) also designed a lid that latched onto the box and could hold a vacuum of up to 50 kPA and positive pressures of up to 10 kPa without minimal deformation. The box also included a port with a pressure gauge attached through which the positive pressure or vacuum could be applied and measured. The ability to apply a vacuum pressure followed by the introduction of carbon dioxide through this top port facilitated saturation of the soil within the box. The box is shown in Figure 2.1 and the lid in shown Figure 2.2.

FIG. 2.1. Model container (box) (Katapa, 2011)

FIG. 2.2. Box lid (Katapa, 2011)

2.2.2 Air-Pluviation

Katapa (2011) developed an air pluviation method to create a liquefiable soil deposit in the ASU box (and later in the Schaevitz centrifuge box) that was based on the air-pluviation method employed by Frost (1989). To employ this method, Katapa (2011) built a pluviation device consisting of a funnel attached to a long PVC pipe. The PVC pipe had two screens at the bottom that would disperse and rain down the soil into the model container in a uniform manner. Katapa (2011) found that the density of the soil varied depending on the size of the screens at the end of the PVC pipe and the distance from the bottom screen to the surface of the soil. Katapa (2011) also determined that, while the density of the resulting soil deposit initially increased with increasing fall height, beyond a certain fall height the density of the soil would no longer increase. Katapa (2011) demonstrated that this pluviation technique produced relatively uniform soil deposits of consistent density in the ASU soil box. Figure 2.3 shows the relationship between fall height and the density of Ottawa 20-30 Crystal Silica sand developed by Katapa (2011).

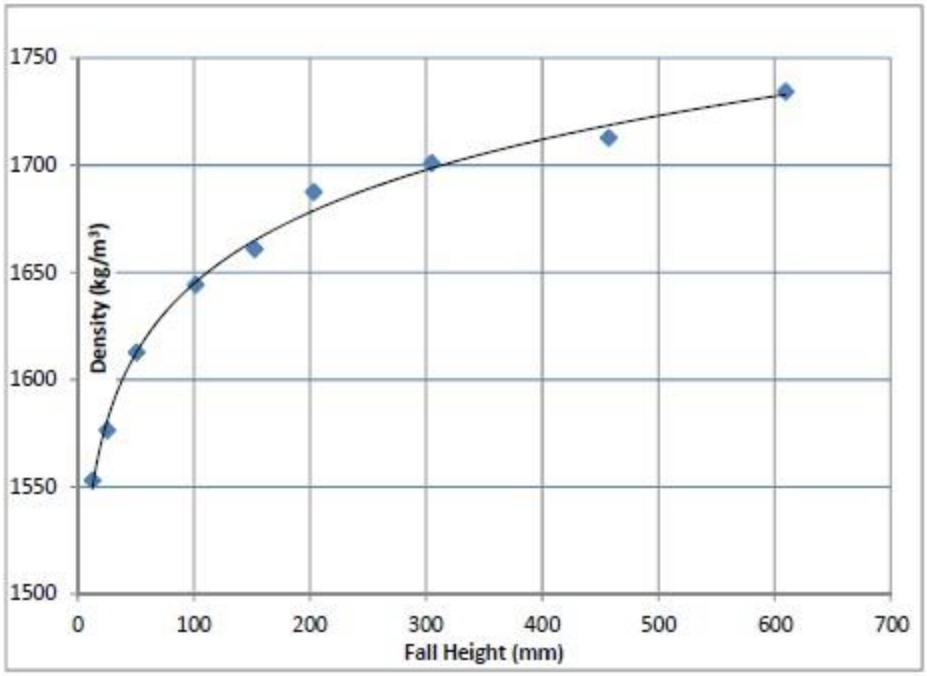

FIG. 2.3. Pluviation fall height-density relationship for Ottawa 20-30 Crystal Silica sand (Katapa, 2011)

2.3 Centrifuge Testing

Centrifuge testing has been employed to study liquefaction for over 20 years. One of the first extensive studies of liquefaction of soil using the centrifuge was the NSF-supported VELACS (Verification of Liquefaction Analysis by Centrifuge Studies) project (Arulanandan and Scott, 1993). The advantage of centrifuge testing is that field-scale stresses can be applied to small scale models in the laboratory. To understand how geotechnical centrifuge testing can be used to mimic field conditions, centrifuge scaling laws must be understood. Kutter (1992) explains the principle of scaling laws in centrifuge testing in a simple fashion. As a model is spun up to a centrifugal acceleration of N times g, where g is the acceleration of gravity at the earth's surface, the dimensions

of the model, are scaled by a factor of N, i.e. the prototype dimension is N times the dimensions of the model, and the pressures and stresses in the model increase by the same factor N. Therefore, the relationship of the model stress to the field, or prototype, stresses can be expressed mathematically by Equation 2.1:

$$\sigma^* = \frac{\sigma_{model}}{\sigma_{prototype}} = 1 \qquad (2.1)$$

where σ is stress, prototype refers to actual conditions, and the asterisk denotes a scale factor for that quantity (Kutter 1992). Thus, in a centrifuge model length is scaled down, gravity is scaled up by the same factor, and stress remains the same. Note that under these conditions mass density in the model remains the same as in the prototype. Scaling factors for other parameters such as earthquake acceleration and pore water viscosity must also be considered in centrifuge testing for liquefaction purposes. Table 2.1 contains the most common scaling factors for geotechnical centrifuge model testing.

Table 2.1. Scale factors for centrifuge model tests (Kutter, 1992).

Quantity	Symbol	Units	Scale Factor
Length	L	L	$1/N$
Volume	v	L^3	$1/N^3$
Mass	m	m	$1/N^3$
Acceleration, Gravity	a, g	L/T^2	N
Force	F	mL/T^2	$1/N^2$
Stress	σ	m/LT^2	1
Moduli	E	m/LT^2	1
Strength	s	m/LT^2	1
Time (dynamic)	t_{dyn}	T	$1/N$
Frequency	F	$1/T$	N
Time (diffusion)[a]	t_{dif}	T	$1/N^2$

An important scaling factor for liquefaction testing in soils is diffusion time, i.e. the rate at which pore pressures will dissipate. Pore water dissipation is a crucial factor in the liquefaction potential of soil. If pore water pressure dissipates too quickly in the soil, the soil will not liquefy. As the scaling factor for diffusion time is $1/N^2$, this can present problems for centrifuge testing where pore pressure diffusion rate must be modeled. The solution used by many researchers, e.g. Dobry et. al (1995) and Kutter (1992), is to use a pore fluid with a viscosity N^2 times that of water. This would allow for similitude between the rate of dissipation of the pore fluid in the model and in the field.

2.4 Acquisition of Undisturbed Samples

Katapa (2011) developed a method for acquiring relatively undisturbed samples of cohesionless soils from the ASU soil box and the Schaevitz rigid box using freezing and coring. A metal pan with a flat bottom was placed on the surface of the soil in the box, in intimate contact with the soil. The pan was filled with 200 proof alcohol and dry ice to create a freezing front that propagated outwards from the bottom of the pan. The pan was slightly smaller than the plan area of box so that a secondary freezing front would not begin to propagate from the aluminum sides of the box. The dry ice and alcohol produced a temperature of -68 degrees Celsius, more than sufficient to advance a freezing front into the soil. The dry ice was continuously replenished as it evaporated in order to keep a constant temperature in the dry ice and alcohol mixture throughout the freezing process. The soil was not allowed to freeze all the way down to the bottom of the container due to problems that were encountered when coring if this was allowed to occur. Katapa (2011) determined that a space of about 25 mm was needed between the bottom of the freezing front and the bottom of the soil box to mitigate potential problems when coring. To leave this thickness of unfrozen soil at the bottom of the box it was determined that, depending on the ambient temperature, the pan with the dry ice and alcohol in it had to be left in place for about 3 to 5 hours.

Katapa (2011) also developing a coring procedure for obtaining the soil samples. Cores of 35 mm (nominally 1.4 inch) and 70 mm (nominally 2.8 inch) diameter were acquired by Katapa from the frozen soil mass. The 35 mm cores were acquired using a 37.5 mm diameter diamond core barrel bit and a Milwaukee 6.35 mm Magnum Drill. The 70 mm cores were acquired using a Husqvarna DR 150 Core Drill Rig and a 71 mm

diameter barrel bit. The 71 mm barrel bit used was a 3 inch-diameter Shelby tube that was modified in order to use it as a bit for the Husqvarna DR 150 Core Drill Rig. Katapa (2011) stated that in order to acquire good cores the coring procedure must not stop once started. Stopping in the middle of the drilling procedure resulted in the coring bit freezing into the soil mass. Once the drill bit reached the unfrozen soil in the bottom of the box, the drilling bit could be removed with the frozen core inside. The frozen core was subsequently extruded from the barrel and preserved for stabilization by wrapping it in foil and placing it in a freezer.

2.5 Stabilization of Soil Samples

Czupak (2011) developed a procedure for stabilization of the frozen soil specimens recovered by Katapa (2011) for subsequent imaging. Stabilization consisted of first thawing the frozen specimen, then drying it, and then impregnating it with optical grade epoxy. The setup used by Czupak (2011), illustrated in Figure 2.4, was modified from a triaxial compression test cell. The steps for thawing the samples were:

1. Place the frozen specimen in the triaxial cell.
2. Apply a 50 kPa confining pressure to the specimen.
3. Apply an additional 15 kPa top cap pressure to the specimen.
4. Let the specimen thaw for a couple hours.
5. Expel the free water from the sample by applying air pressure through the top cap and forcing the water out through the line on the base of the cell, collecting the water into a glass beaker.
6. Discard the water that was collected.

7. Clean the beaker, add 99.9% isopropyl alcohol to the beaker, and place it in the pressure chamber.
8. Apply pressure to the chamber to push the alcohol through the sample from the bottom up, collecting and discarding the alcohol as it comes out of the system.

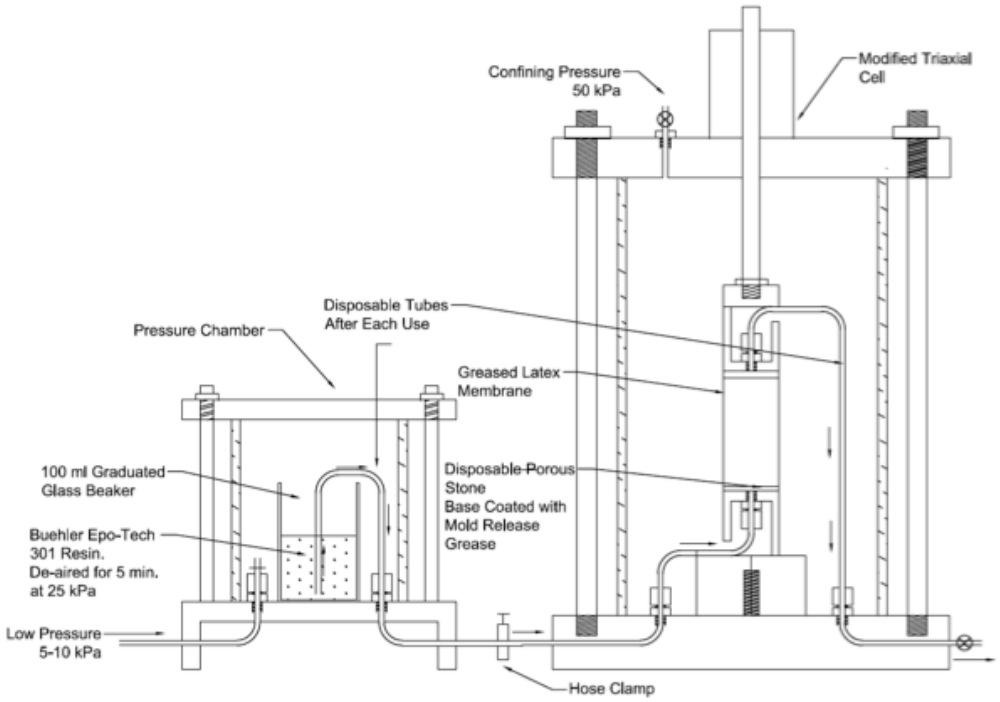

FIG 2.4 Modified triaxial cell setup (Czupak, 2011)

The setup used by Czupak to finish drying the thawed specimen (after flushing it with alcohol) is shown in Figure 2.5. A gauge was connected to the vacuum chamber to measure the relative humidity of air pulled by vacuum through the pore space. Next, a silica gel (SiO_2) desiccant was placed on the top cap line of the system. A vacuum of 15 kPa was then applied to the specimen to dry out the sample by pulling air first through the desiccant and then through the specimen. The humidity gauge was monitored until the relative humidity of the air pulled through the specimen dropped below 10%.

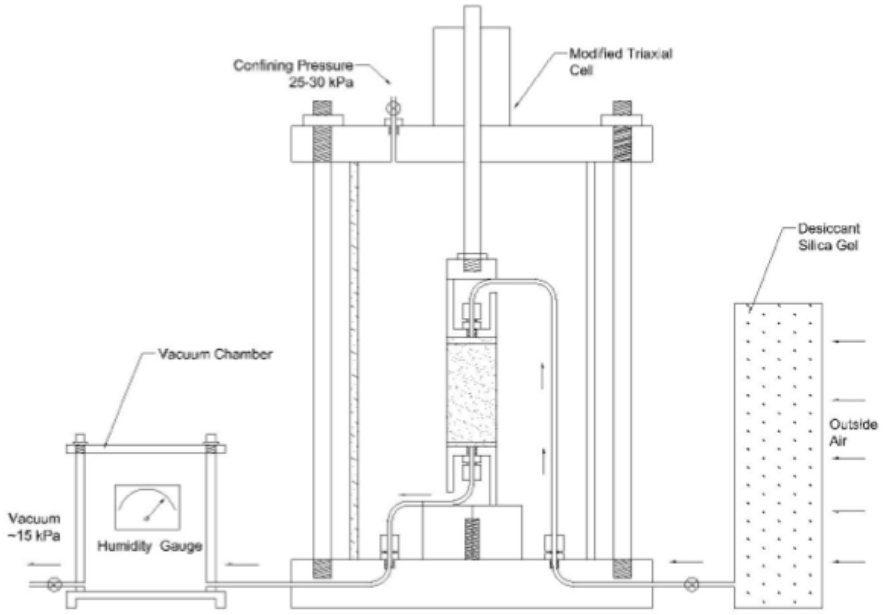

FIG 2.5 Specimen drying setup (Czupak 2011)

Once the desired relative humidity was reached, the specimen was ready for impregnation.

Czupak (2011) used Buehler® Epotek 301 two part optical grade epoxy to impregnate the sample. About 32 to 35 mL of epoxy was required for complete impregnation of a 1.4 inch diameter, 2.8 inch high specimen. The epoxy was mixed in 25 mL batches in accordance with the specifications provided by the manufacturer. The epoxy was dispensed into a disposable 118 mL jar using graduated pipettes to achieve the correct part A-to-part B ratio as specified by the manufacturer. The epoxy was then mixed thoroughly for 2 minutes until it showed a uniform consistency and was clear to the eye. Air entrained in the epoxy by the mixing process that could cause problems in imaging was removed from the mixture using the vacuum degas method recommended by the manufacturer. According to Epotech Technical Data (2009), a vacuum pressure of

at least 98.2 kPa is needed along with a container that is at least 5 times larger than the epoxy volume. Czupak applied a 172 kPa vacuum pressure to the 118 mL jar that was sealed and allowed the vacuum to remove all the air bubbles from the epoxy. The deairing process ran anywhere from 5 to 8 minutes until all of the visible bubbles were forced out of the solution epoxy. Once the epoxy was degassed, the 118 mL beaker containing deaired epoxy was placed in the vacuum chamber and a pressure of 7 - 14 kPa was applied to the chamber to push the epoxy into the specimen at a very slow rate (in order to minimize disturbance of the soil structure). Once the entire 25 mL of epoxy was introduced into the specimen, the inflow tubing was clamped to prevent it from draining out and the 118 mL beaker was replenished with an additional 7 mL of deaired epoxy. The remaining 7 mL of epoxy were then introduced into the specimen and the tubing was again clamped to avoid draining. The epoxy was then allowed to set for 24 hours at room temperature.

2.6 Soil Imaging

2.6.1 Bright Field Microscopy Imaging of Stabilized Soil specimens

Czupak (2011) employed bright field microscopy (BFM) to image an Ottawa 20-30 soil specimen stabilized using Epo-Tek® 301 epoxy in order to determine the local void ratio distribution . The BFM procedure used by Czupak (2011) was based upon the procedure developed by Frost and Kuo (1996). A 1 cm coupon was cut from the stabilized soil sample and was meticulously polished. The polished coupon was imaged using an optical microscope with a built-in light source connected to a digital camera and

personal computer (Czupak 2011). The images were taken using an InfiniVar CFM-2/S microscope (www.infinity-usa.com).

The imaging procedure consisted of taking a number of individual images each about about 7 mm x 5 mm in size. These images were then stitched together using the Panavue Image Assembler™ software (www.panavue.com) to recreate the whole surface of the coupon. The images were then processed using ImageJ, an open source software package (http://rsbweb.nih.gov/ij/) to determine the local void ratio distribution. The flow diagram developed by Czupak (2011) to describe the image processing method is presented in Figure 2.6.

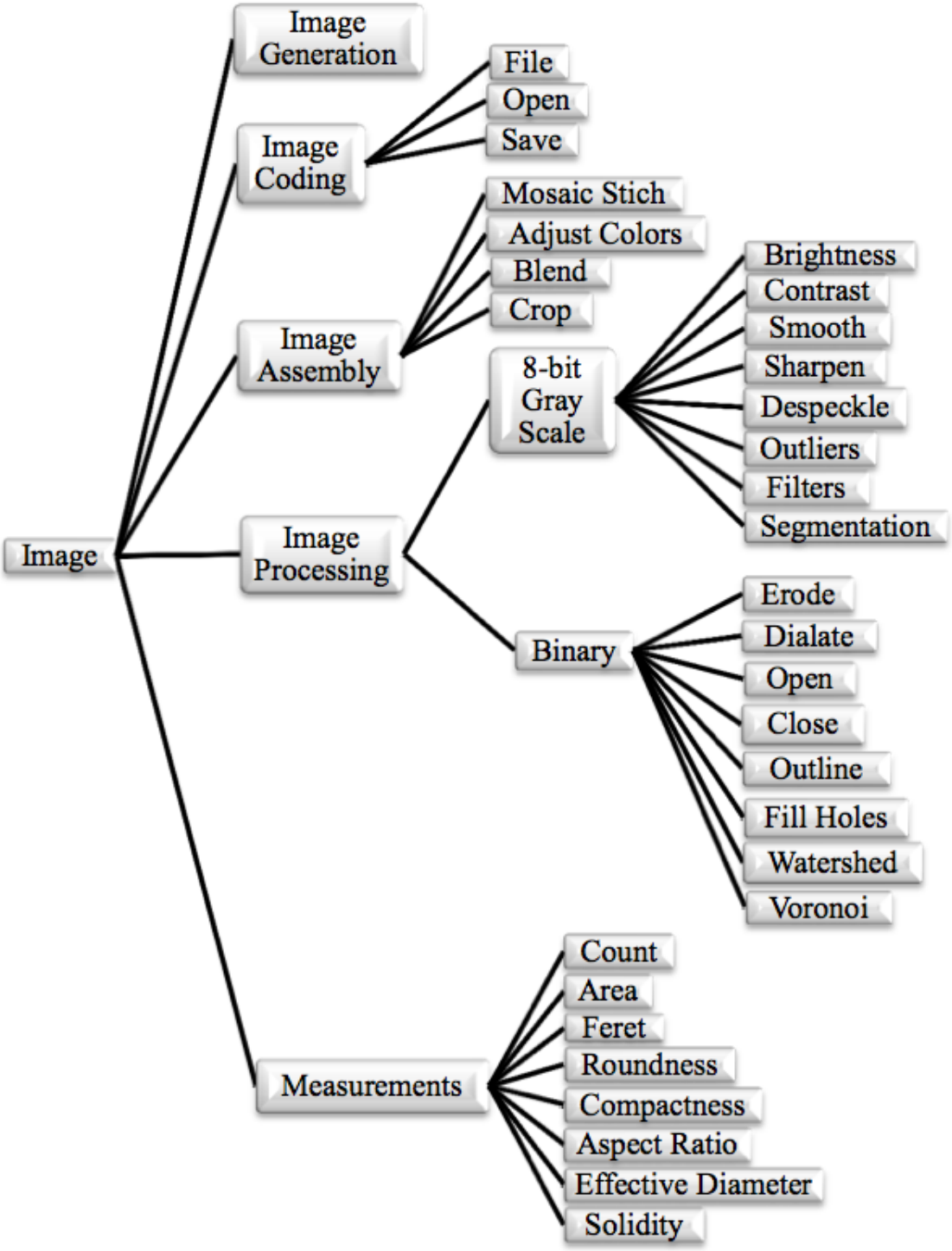

FIG. 2.6. Work flow diagram for image processing. (Czupak, 2011)

Czupak (2011) established a representative coupon size of 10 mm by 10 mm for image analysis of the specimen. He determined this based on statistical analyses based on the deviation of localized void ratios from the global void ratio. He calculated a void ratio equal to .5470 by measuring the mass of the soil as he was placing it in the sample and determining the density in this manner. The void ratio determined from the air pluviated stabilized samples was .5475. Finally, his void ratio for the air-pluviated and frozen samples was calculated to be .5455.

Czupak (2011) developed plots that showed standard deviation versus sample size of the void ratio distribution. Figure 2.7 shows the plots developed by Czupak which show how as the representative sample size increases, the standard deviation from the global mean decreases. Czupak (2011) concluded that a representative coupon size for image analysis and processing should be at least 10 mm by 10 mm and should contain between 200 and 250 grains in order for the void ratio of each individual coupon to be representative of the void ratio of the entire specimen.

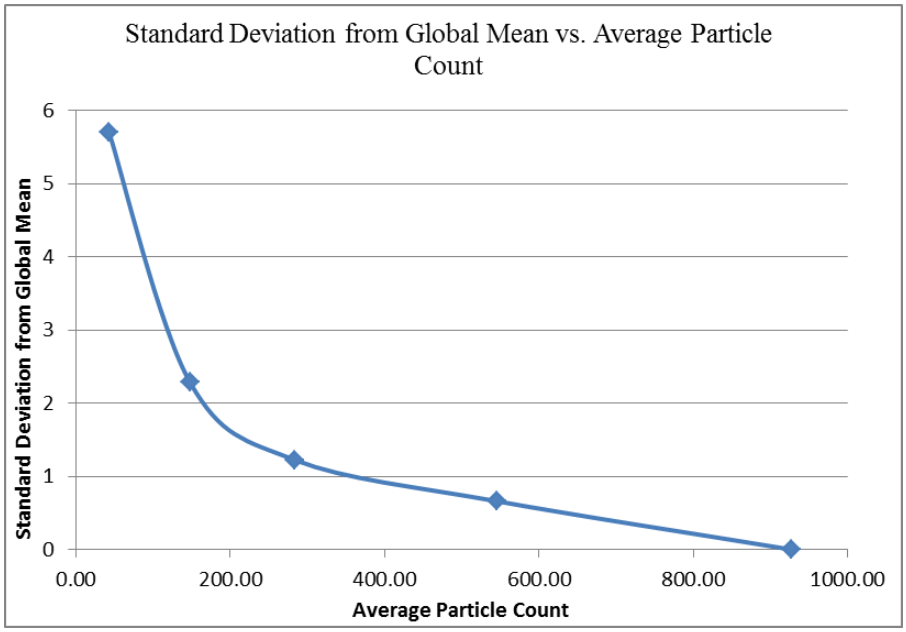

FIG. 2.7. Standard deviation vs. average particle count. (Czupak, 2011)

2.6.2 CT Scan Imaging of Soils

X-ray Computed Tomography is a non-destructive imaging method that takes a number of two-dimensional images or slices of density contrast throughout a material and stitches them together to create a three dimensional representation of the material density. This method has been used in the medical industry for a number of years. It has also been used to image geological media, including soil specimens. Two of the studies on soil specimens most applicable to this dissertation were done by Batiste et. al (2004) and Al-Raoush and Alshibli (2006).

Batiste et. al (2004) studied shear bands in Ottawa F-75 sand specimens that were subjected to triaxial testing. These researchers used CT imaging to analyze shear band thickness and orientation, local void ratio distribution, and volume change distribution in

triaxial test specimens before and after shearing. Batiste et. al (2004) concluded that CT is an excellent method for quantifying void ratio distribution within a soil specimen.

Al-Raoush and Alshibli (2006) also used CT to evaluate porous media systems. In their research they created a three dimensional representation of a soil sample from the CT scan images. They then developed a method to determine the local void ratio distribution from these three-dimensional models. An advantage of their methodology was that it was not affected by geometrical irregularities within the porous media such as shape, size, and arrangement of the particles. They found that calculated void ratios in the porous media system were affected by the quality of the images and that image filtering should be done prior to calculation of the local void ratio distribution to get accurate results. Therefore, they created a number of image filter algorithms to analyze the scans. These image filters were used to segment the image to separate overlapping particles and calculate local void ratios.

2.7 Stress-Strain of Ottawa 20-30 Crystal Silica Sand

Katapa (2011) evaluated the stress-strain behavior of Ottawa 20-30 crystal silica sand. He conducted undrained triaxial tests on frozen and never-frozen Ottawa 20-30 to determine if the stress-strain properties of the soil would change due to freezing and thawing. Katapa (2011) conducted a total of 5 undrained triaxial tests on Ottawa 20-30 crystal silica sand at a relative density of between 80 and 82 percent to establish baseline stress-strain behavior. Table 2.2 shows the initial properties of the undrained baseline specimens tested by Katapa (2011). The results for his undrained triaxial tests on these specimens are presented in Figure 2.8

Table 2.2 Initial properties of undrained baseline test specimens. (Katapa, 2011)

Test #	Sample Height (mm)	Mass of Sand (g)	Initial Density (kg/m^3)	Relative Density (%)
1	150	1019	1710	80
2	149	1013	1712	81
3	150	1012	1714	82
4	150	1019	1710	80
5	149	1012	1710	80

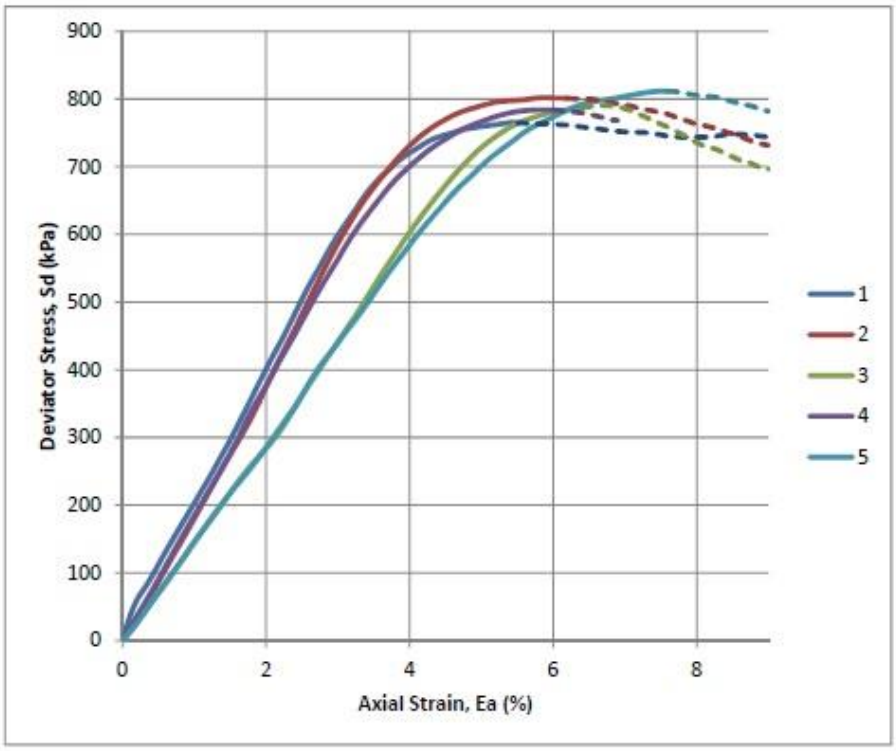

FIG. 2.8. Undrained stress-strain response of Ottawa 20-30 sand baseline specimens. (Katapa, 2011)

To compare the results of his baseline tests to tests on frozen and thawed specimens, Katapa (2011) developed a confidence interval from the baseline curves. The confidence interval was bound at the top by the mean plus two standard deviations and bound at the bottom by the mean minus two standard deviations curves developed from the baseline tests. Katapa (2011) plotted results from undrained tests on three frozen and then thawed specimens against the confidence interval developed from the baseline tests. Because, as shown in Figure 2.9, the stress-strain curves from the frozen nd thawed specimens all fell within the confidence bounds from the baseline tests, Katapa (2011) concluded that his procedure for freezing, coring, and thawing specimens yielded relatively undisturbed specimens of Ottawa 20-30 sand.

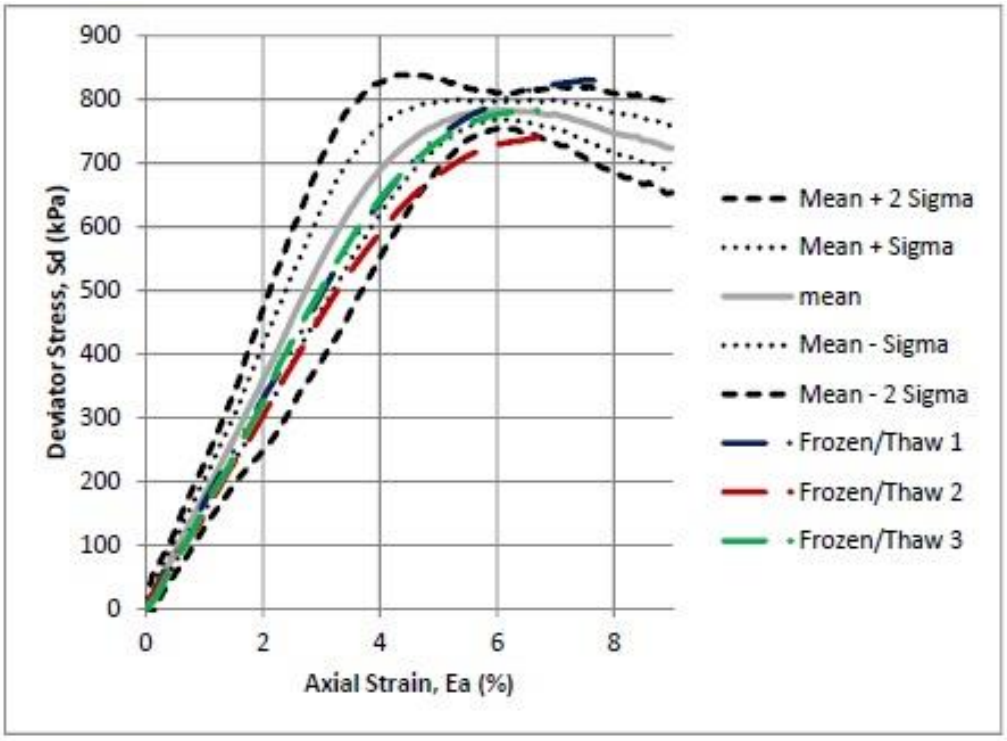

FIG 2.9. Undrained stress-strain-strength results plotted on confidence interval developed from the baseline undrained triaxial tests (Katapa, 2011).

Chapter 3

3 RESEARCH PROGRAM

3.1 Introduction

The research program described in this thesis included the following activities:

- Laboratory testing to establish baseline geotechnical properties of the soils employed in the models;
- Pluviation and sedimentation of liquefiable soil deposits in the rigid container for the small Schaevitz centrifuge at UC Davis and the ASU model box, respectively, followed by liquefaction of soil in the UC Davis box using the centrifuge and in the ASU model box using a shaking table;
- Recovery and stabilization of cores recovered from UC Davis and ASU model boxes before and after liquefaction;
- X-Ray CT scanning of the same specimen used by Czupak (2011), processing of the scans to quantify local void ratio, and comparison from the processed CT scans to results obtained by Czupak (2011) using optical microscopy to establish that similar results were obtained using the two different methods (CT and optical microscopy);
- X-Ray CT scanning of stabilized cores followed by processing of the CT scans to quantify the local void ratio distribution in the stabilized cores followed by comparison of local void ratio distributions on cores recovered before and after liquefaction.

Each of these activities is described in additional detail in the subsequent sections of this chapter.

3.2 Soils Employed in the Research

Two different materials were employed in the research program: Ottawa 20-30 Crystal Silica Sand and Ottawa F60 Crystal Silica Sand from US Silica Company's Ottawa, Illinois, source. The soils are referred to herein as Ottawa 20-0 (or just 20-30) and Ottawa F60 (or just F60) sand. Initially, testing was conducted using the 20-30 sand, the same soil employed by Katapa (2011) when he developed the ASU soil model box and associated sample preparation and core recovery procedures and by Czupak (2011) when he developed core stabilization and optical imaging procedures to obtain local void ratio distribution. Due to the difficulty in liquefying the 20-30 sand in the initial centrifuge tests, subsequent centrifuge tests were conducted using the F60 sand. However, the 20-30 sand was employed in the shaking table test conducted to liquefy soil in the ASU model box.

3.2.1 Ottawa 20-30 Sand

Ottawa 20-30 is a poorly graded, subrounded sand with a mean grain size of 1 mm. The grain size distribution curve in Figure 3.1 from Czupak (2011) shows the poorly graded nature of the Ottawa 20-30 sand. According to the U.S. Silica Company (2011), 99.8% of the material is quartz and 1 percent is retained in the number 20 sieve, 97 percent of the material is retained on the number 30 sieve, and the rest passes the number 30 sieve.

The maximum and minimum void ratios for Ottawa 20-30, along with many other soil properties, were studied by Santamarina and Cho (2001) and summarized by Czupak (2011). The summary table prepared Czupak (2011) is provided below as Table 3.1. Appendix A shows the product data sheet for Ottawa 20-30 Crystal Silica Sand.

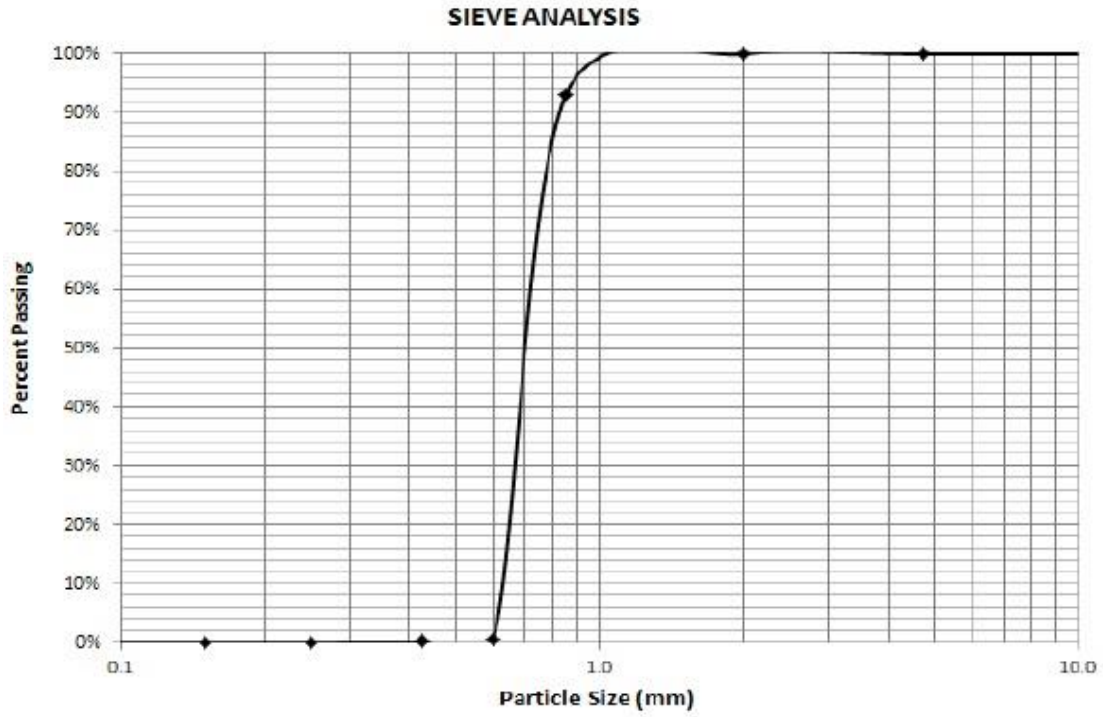

FIG. 3.1. Grain size distribution for Ottawa 20-30. (Czupak 2011)

Table 3.1. Physical characteristics of Ottawa 20-30 (Czupak 2011).

PARAMETER	VALUE	REFERENCE
D_{10}	0.65 mm	Santamarina and Cho (2001)
D_{50}	0.72 mm	Santamarina and Cho (2001)
e_{max}	0.742	Santamarina and Cho (2001)
e_{min}	0.502	Santamarina and Cho (2001)
C_u	1.15	Santamarina and Cho (2001)
C_c	1.02	Santamarina and Cho (2001)
G_s	2.65	Santamarina and Cho (2001)
φ_{cr}	28° (undrained)	Santamarina and Cho (2001)
Slope of CSL in e log p'	0.053 (undrained)	Santamarina and Cho (2001)
D_{10}	0.64 mm	ASTM D422
D_{30}	0.66 mm	ASTM D422
D_{50}	0.70 mm	ASTM D422
D_{60}	0.72 mm	ASTM D422

3.2.2 Ottawa F60

Ottawa F60 Crystal Silica sand is also from the Ottawa, Illinois source used by the US Silica Company. F60 sand consists of white, round sand particles mostly comprised (99.8%) of quartz (US Silica Company 2011). The mean grain size of F60 sand is 0.25 mm. Figure 3.2 shows the grain size distribution for Ottawa F60. The maximum and minimum void ratios for F60 were determined according to ASTM D4254. Table 3.2 shows the maximum and minimum void ratios along with selected physical properties of F60. These properties were taken from the Ottawa F60 Silica sand product fact sheet found in Appendix B.

Table 3.2. Physical characteristics of Ottawa F60.

PARAMETER	VALUE
e_{max}	.8315
e_{min}	.6014
D_{10}	.15 mm
D_{30}	.19 mm
D_{50}	.23 mm
D_{60}	.26 mm
C_u	1.73
C_c	.926
G_s	2.65

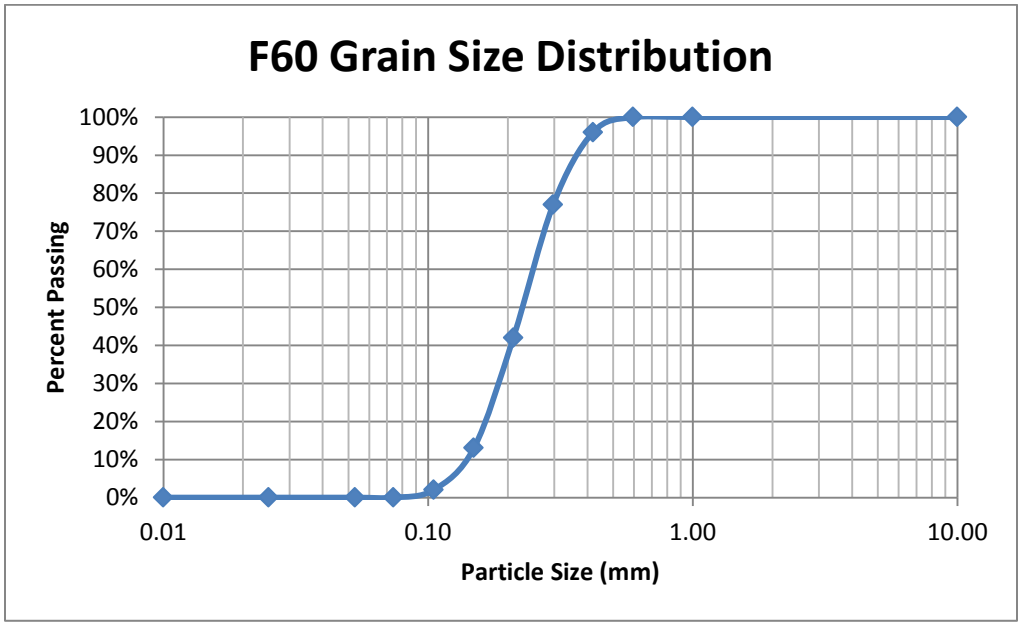

FIG. 3.2. F60 grain size distribution.

3.3 Model Preparation Methods

Two different methods were used to prepare the models for the liquefaction experiments. One method was used to prepare deposits of Ottawa 20-30 and F60 sand for testing in the UC Davis centrifuge while the second method was used to prepare deposits of Ottawa 20-30 sand for testing on the ASU shake table. For the centrifuge tests, the air-pluviation developed by Katapa (2011) and the UC Davis saturation procedure for centrifuge model testing were employed. The shake table tests employed sedimentation through water to create a saturated soil deposit.

3.3.1. Centrifuge Model Preparation

Models of liquefiable soil deposits for testing on the UC Davis Schaevitz centrifuge were prepared using air pluviation. The air-pluviation method used for centrifuge model preparation was based on the method developed by Katapa (2011).

The pluviation device employed for model preparation for centrifuge models that employed Ottawa 20-30 sand was the Katapa (2011) pluviation device. A fall height of about 21 mm was used to achieve a relative density of approximately 60% within the model box.

The pluviation device employed for model preparation for F60 models was the Katapa (2011) pluviation device with modified screens. The screens used for the F60 pluviation device were built out of 1/16" contour mesh. The minimum feasible fall height, a fall height of about 1 mm, was used to achieve a relative density as low as feasible within the model box. The lowest relative density that could be achieved with this procedure within the rigid box at UC Davis was 53%. The test soil was pluviated

until the sand completely filled the box. The surface of the soil deposit was then contoured using a mold and a vacuum to create a curve that had a radius of curvature that corresponded to the "gravity" field induced a centrifuge test.

Centrifuge models were instrumented using accelerometers, a linear variable displacement transducer (LVDT), and pore pressure transducers. The LVDT was placed below the box, attached to both the arm and the box. This allowed for measurement of actual displacement of the box within the centrifuge arm. Transducer placement within the model followed the procedures developed by UC Davis for centrifuge model testing. At least one accelerometer was used for each test. The accelerometer was placed on the side of the rigid box to keep track of the input motion. When additional accelerometers were used, they were placed within the soil deposit. Pore pressure transducers were also placed within the soil deposit in the centrifuge tests that employed Ottawa 20-30 sand. However, due to concern over damaging the pore pressure transducers when the soil was frozen, only older, expendable pore pressure transducers were sued and the results were not considered reliable. Therefore, pore pressure transducers were not employed in the centrifuge tests that used Ottawa F-60 sand.

The transducers, internal accelerometers, and pore pressure transducers (when used) were placed either in the center of the model or in the corners. Transducers were placed by pluviating above the desired elevation of the transducer, using a vacuum to vacuum out soil to the desired elevation, placing the transducer, and then pluviating soil back on top of the transducer. Transducer wiring was routed along the soil surface to the side of the box and then up the side wall of the box and held in place with modeling clay. The wiring was then secured to the centrifuge arm and routed up to the control box at the

center of the centrifuge. Some slack was left in the wiring at the box end of the wiring to allow the centrifuge bucket to swing up and not disturb the model or damage the sensors. Two layers of colored sand were placed horizontally in each model to facilitate visual observation of liquefaction phenomena. Once the model was built, it was placed on the centrifuge arm and secured. Figure 3.3 shows a model secured onto the centrifuge arm and ready for spinning.

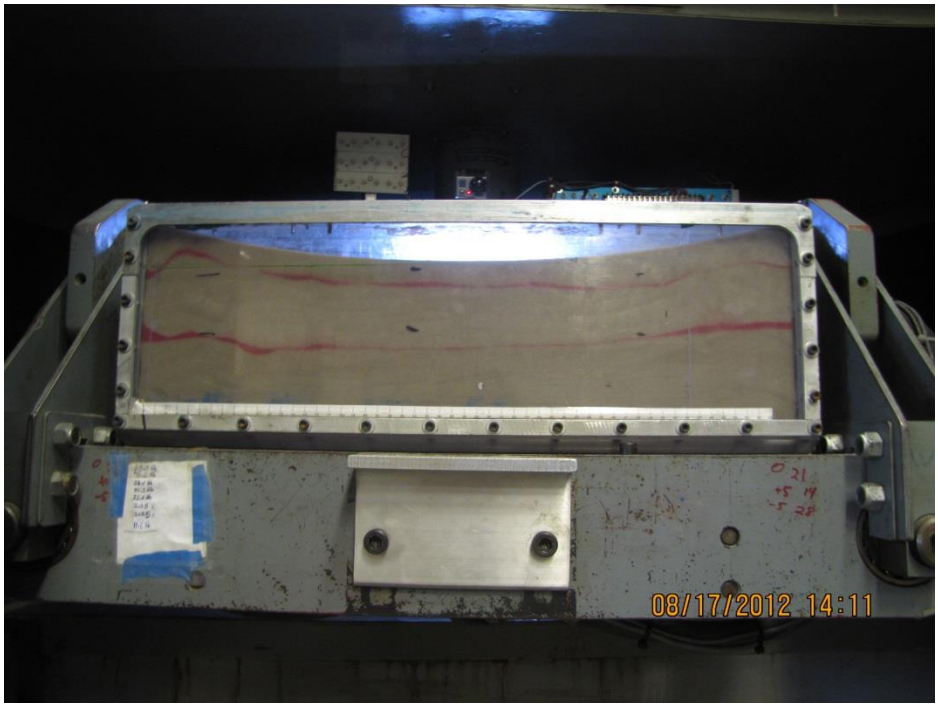

FIG. 3.3. Mounted model ready for centrifuge testing.

The soil model was then saturated according to the standard procedure developed for saturation of sand models in the Schaevitz centrifuge at UC Davis (Ueno, 2000). The box was sealed and a vacuum pressure of 28 psi was applied to the box to remove as much air as possible. The vacuum pressure was then removed from the box and CO_2 was

slowly be introduced into the sample. Once the vacuum pressure was close to 0 psi, the vacuum pressure was slowly increased to 28 psi and the sample was again flushed with CO_2. The vacuum pressure was again increased to 28 psi and deaired water was then very slowly introduced into the model until the water level was above the soil surface. The vacuum pump would be turned off and the sample was allowed to reach a gage pressure of 0 psi very slowly. The lid was then removed from the model. Once the model was saturated, it was ready for testing.

3.3.2 Shake Table Model Preparation

Due to difficulties in liquefying Ottawa 20-30 Crystal Silica sand in the centrifuge, deposits of Ottawa 20-30 sand were subsequently subjected to liquefaction in the ASU laboratory on a shake table. Models of liquefiable soil deposits for testing on the ASU shake table were prepared using sedimentation. Sedimentation instead of air-pluviation was used in the ASU shake table tests to facilitate saturation and because lower relative densities (between 36-42%) than achievable using the air-pluviation method could be achieved using sedimentation. The sedimentation procedure consisted of filling the model box with water about ¾ of the way up. The test sand was then slowly poured into the model. As sand was added, water was displaced and the water level rose. A layer of colored sand was placed in each shake table model at approximately mid-height of the box. Sand was added up to about an inch below the top of the box, at which point the sand model was ready for testing.

3.4 Model Testing

3.4.1 Centrifuge Model Testing

Initially, models were tested using the small Schaevitz centrifuge and the rigid box at the UC Davis Center for Geotechnical Modeling. The 1 m radius Schaevitz centrifuge can spin up to 100 g with a payload of approximately 100 lbs for dynamic (earthquake) testing. The UC Davis Shaevitz centrifuge shaker has the ability to employ a large number of historical earthquake motions and sinusoidal loading to the model box.. Figure 3.4 shows the arm and the bucket of the Schaevitz centrifuge.

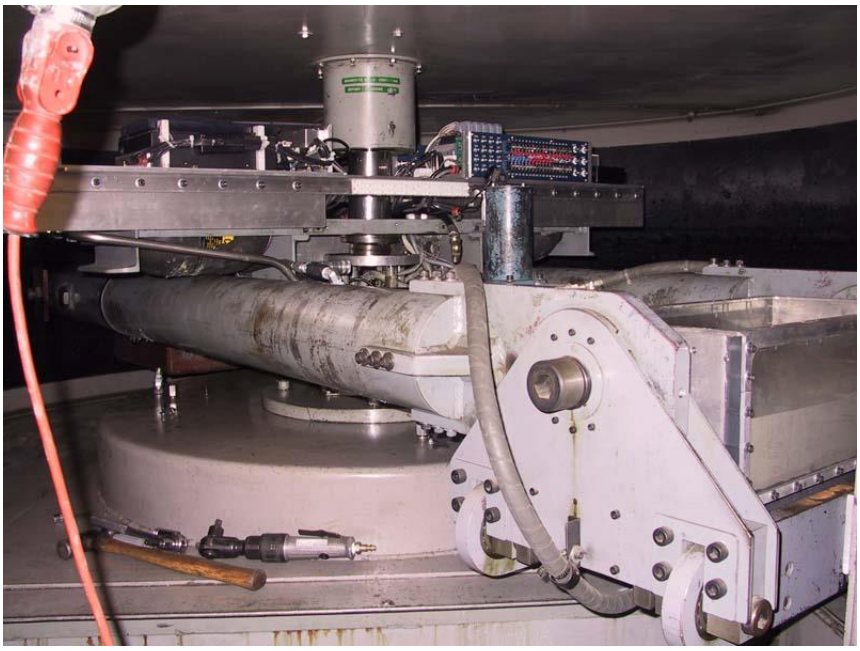

FIG. 3.4. Schaevitz centrifuge. (UC Davis, 2013)

An LVDT was attached to the arm and the bottom of the rigid box to measure the displacement of the box while spinning and shaking. The models was spun up to the desired g level and then subjected to either sinusoidal or earthquake-like accelerations in

one of the horizontal model directions. The centrifuge was then spun down and the model was removed. After spinning down the centrifuge and removing the model, the soil in the model was frozen by placing a pan containing dry ice and alcohol on the surface of the model and cores were recovered using the techniques developed by Katapa (2011). The cores were then transported to ASU for stabilization with epoxy using the technique developed by Czupak (2011).

3.4.2 Shake Table Testing

Due to difficulties encountered during centrifuge testing, soils were also liquefied using a small shaking table in the ASU soils laboratory. The shaking table was constructed using a direct shear actuator, a flat steel plate, and roller bearings. The actuator was connected to the ASU soil box and the soil box was placed on top of the steel plate with the roller bearings between the plate and the bottom of the box. This set-up was capable of applying a sinusoidal displacement (A) of 0.75 mm at a frequency (ω) of 62.83 radians (10 cycles) per second, resulting in an acceleration of 0.3 g on the box. The model for the shake table test was built using the sedimentation method described in the previous sections. The shake table model was constructed with the box on the shake table and then subjected to approximately 70 cycles of sinusoidal loading as described above (0.75 mm amplitude, 10 Hz frequency, 0.3 g peak acceleration). Monitoring of the shake table test was purely visual and consisted primarily of observations of sand boils identified based upon expelling of colored sand at the ground surface. After shaking the model and allowing the excess pore pressures to dissipate, the soil was frozen and cores were recovered using the techniques developed by Katapa (2011). The cores were then

stabilized with epoxy using the technique developed by Czupak (2011). Figure 3.5 shows the shake table apparatus.

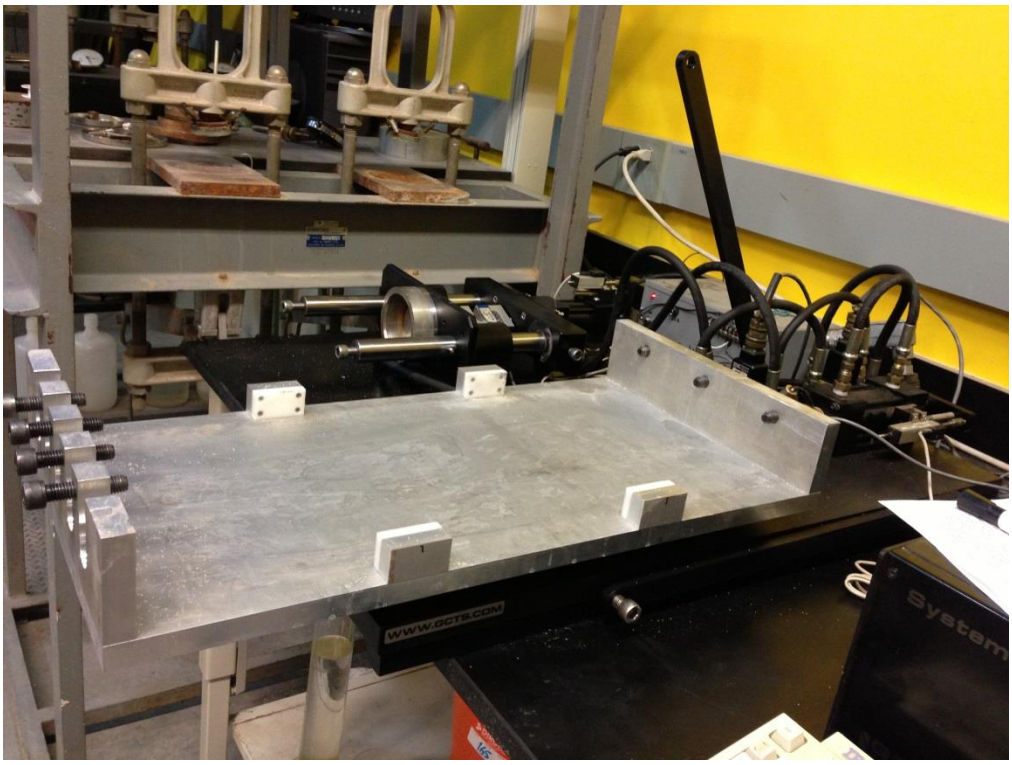

FIG. 3.5. Shake table apparatus.

3.5 X-Ray CT Scans

Stabilized samples were sent to the NSF-sponsored X-ray Computed Tomography Facility at the University of Texas Austin for high-resolution CT scanning. This CT facility is an NSF funded multi-user facility used primarily for high resolution imaging of geological media. The samples sent to UT Austin for imaging included the stabilized core on non-liquefied Ottawa 20-30 sand used by Czupak (2011) for his optical imaging work, and cores from non-liquefied and liquefied soil deposits from the centrifuge and

shake table models. The CT scan images acquired from UT Austin were 1024 X 1024 16-bit TIFF images. The slice thickness of each of the images was 0.03867 mm.

3.5.1 CT Scan Image Analysis

16-bit grayscale images of the epoxied stabilized cores taken using computed tomography were analyzed for local void ratio distribution using Avizo® Fire. The images were analyzed not as a single 2D image but rather as a stack of images that provided a 3D representation of the specimen. This was done using a randomly selected small number of image slices (typically about 13) and working with them as representative of the entire specimen. To open a number of slices and build a 3D representation of the model all that has to be done in Avizo® Fire is to select the desired images when opening the data. This automatically creates a 3D model as long as the images are selected in order and are in a format that Avizo® Fire can work with. While the use of 13 slices in this procedure created a 3-D image, the thickness of the image (0.467 mm) was somewhat less than the Ottawa 20-30 particle thickness (about 0.70 mm) and so it still provided an essentially 2-D representation of the Ottawa 20-30 soil particle distribution.

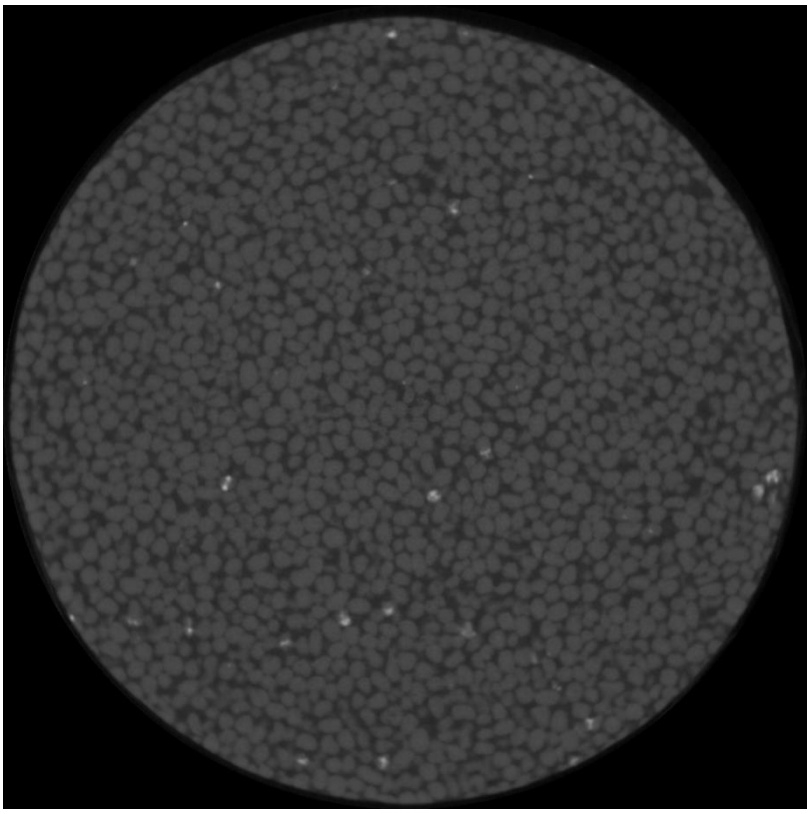

FIG. 3.6. Unprocessed CT scan image of a soil specimen.

The first step in the image analysis procedure was to extract a *subvolume* of the specimen. The size of the *subvolume* is determined by the analyst. Once the *subvolume* was selected, an *ortho-slice* is taken for each of three orthogonal axes in the subvolume and various filters are applied to observe the effects of the filters on the image analysis results. Since the CT scan images were not taken at very high resolution, these filters were required to sharpen the images. Different *subvolumes* required different filters according to the needs for that particular *subvolume*. The most common filters used for analyses were *medianfilter3D*, *Brightness-Contrast*, and *Gamma Correction*. Once the *subvolume* was filtered to the desired quality, the *logical_not* quantification tool was used to select the soil particles. The *logical_not* quantification tool changes the main focus of

the image from the voids to the soil grains. This tool was used because it was easier to filter and analyze the soil grains in later steps of the procedure.

Next, the *I_threshold* tool was used to determine which grayscale range will be employed as the separation point between particles and void space for the binary image when turning the grayscale image into a binary image. The threshold that was employed once again varied depending on the quality of the image and the contrast between the soil grains and void space. This step is crucial in the quantification of local void ratio as not choosing a proper threshold value will result in erroneous results. The threshold must be decided by the analyst on a *subvolume* by *subvolume* basis. The selection of the threshold value is based on creating a proper contrast between the soil grains and the void space. The quantification tool *binseparate* was then used to create separation between the soil particles where the particles seemed to overlap. The quantification tool *I_analyze* was then used to analyze the volume of the soil particles. The *I_analyze* tool can be used to quantify many different parameters describing the soil grains, including most importantly the volume for each soil particle. The *logical_not* tool was then used to switch the focus of the analysis back to the void space. This allows for the use of the *I_analyze* tool to calculate the volume of the void space of the *subvolume*. Once the volume of soil solids and the volume of void space are known, the void ratio can be calculated. The void volume calculated in this manner was compared to the total volume of the *subvolume* minus the calculated volume of soilids and the void ratio calculated in this manner was compared to the void ratio calculated using the specimen mass and specific gravity as a check on the image processing procedure (i.e. to make sure no volume was lost during processing). A flow chart for the basic imaging analysis

procedure is presented in Figure 3.7. Figure 3.8 shows a *subvolume* of a soil specimen that has been through the image analysis procedure.

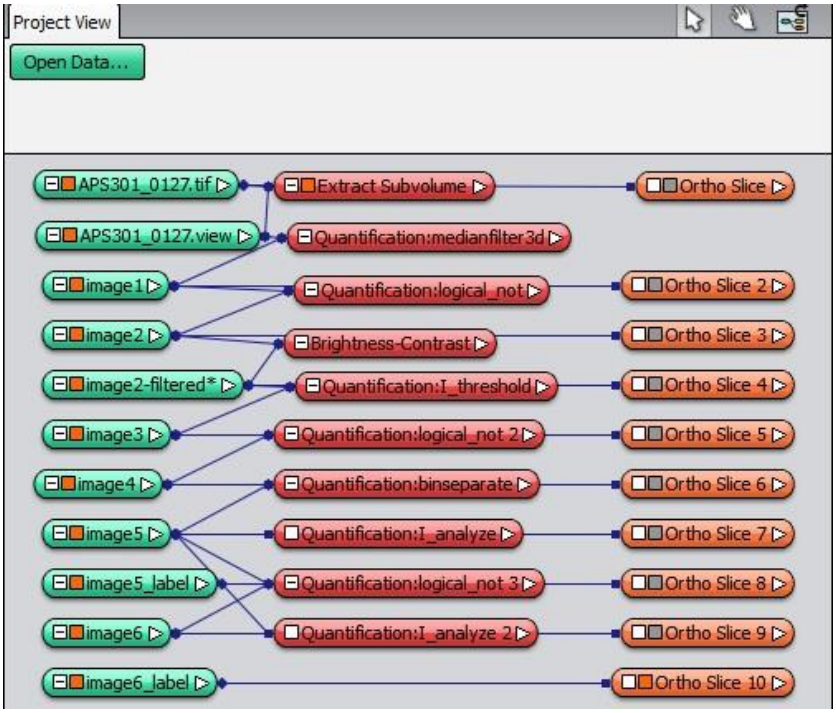

FIG. 3.7. Avizo® Fire procedure.

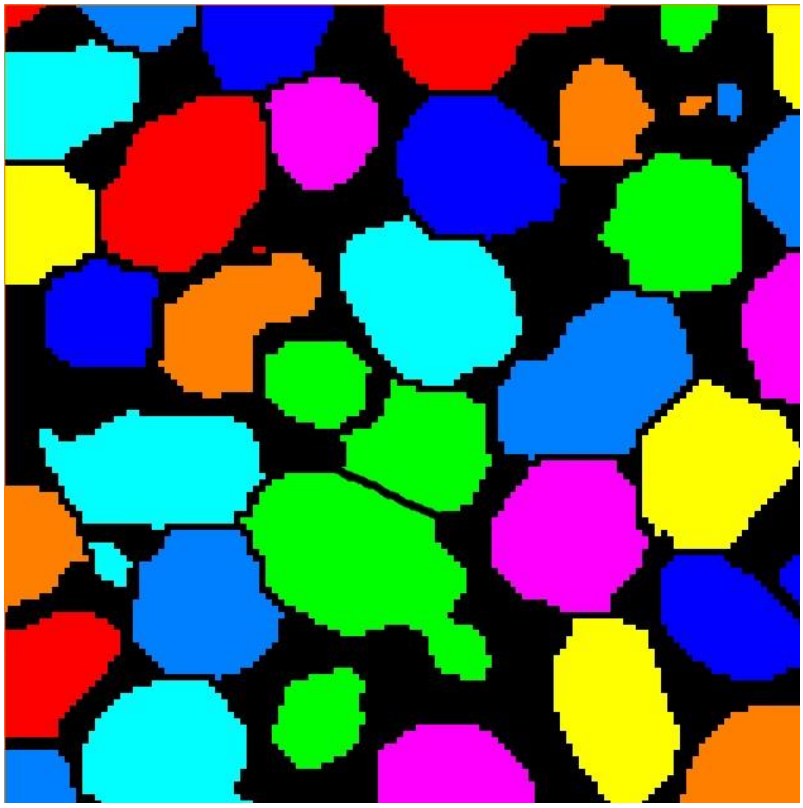

FIG. 3.8. Filtered subvolume of a soil specimen.

3.5.2 Importance of Thresholding

Thresholding within the image analysis procedure, discussed in section 3.5.1, is the most crucial step. The thresholding quantification tool is used to determine the range of gray within the grayscale image should be selected as void space and what range of gray within the grayscale image should be considered soil particles. The ideal thresholding range would have two distinct peaks within the grayscale histogram. Two distinct peaks were not acquired in most images but thresholding was still possible by balancing the grayscale range within the two peaks and getting an optimal level for a slice. Figure 3.9 shows an example of a bad histogram for thresholding while Figure 3.10 shows a better histogram for thresholding.

FIG. 3.9. Low quality histogram for thresholding.

FIG. 3.10. Higher quality histogram for thresholding.

Chapter 4

4 MODEL TESTING

4.1 Test Soils

Two methods were used to create for the models used in this study. One method consisted of sedimenting Ottawa 20-30 Crystal Silica sand in the model box. The second method consisted of pluviating Ottawa F60 Silica sand into the model box . This section describes the baseline properties of specimens prepared using these two methods.

4.1.1 Ottawa 20-30

Ottawa 20-30 Crystal Silica sand was placed in the model box using the sedimentation process. The sedimented soil had a relative density of 36% as calculated by measuring the volume of the box, keeping track of the amount of sand that was being poured into the sample, and using the equation for relative density below:

$$D_r(\%) = \frac{e_{max} - e}{e_{max} - e_{min}} * 100 \qquad \textbf{(4.1)}$$

where D_r is relative density, e is the measured void ratio, and e_{max} and e_{min} are the maximum and minimum void ratios published by Santamarina and Cho (2001) for Ottawa 20-30 Crystal Silica sand.

The shear strength of the Ottawa 20-30 Crystal Silica sand was evaluated by triaxial testing . Both drained and undrained triaxial tests were conducted on Ottawa 20-30 sand. Figure 4.1 shows the stress-strain curves and pore pressure response for two undrained triaxial tests on Ottawa 20-30 sand pluviated to a relative density of 60% and a

confining pressure of 60 kPa. Figure 4.2 shows the stress-strain curve and volumetric strain for a drained triaxial test on Ottawa 20-30 sand prepared by sedimentation at a relative density of 36% and a confining pressure of 100 kPa.

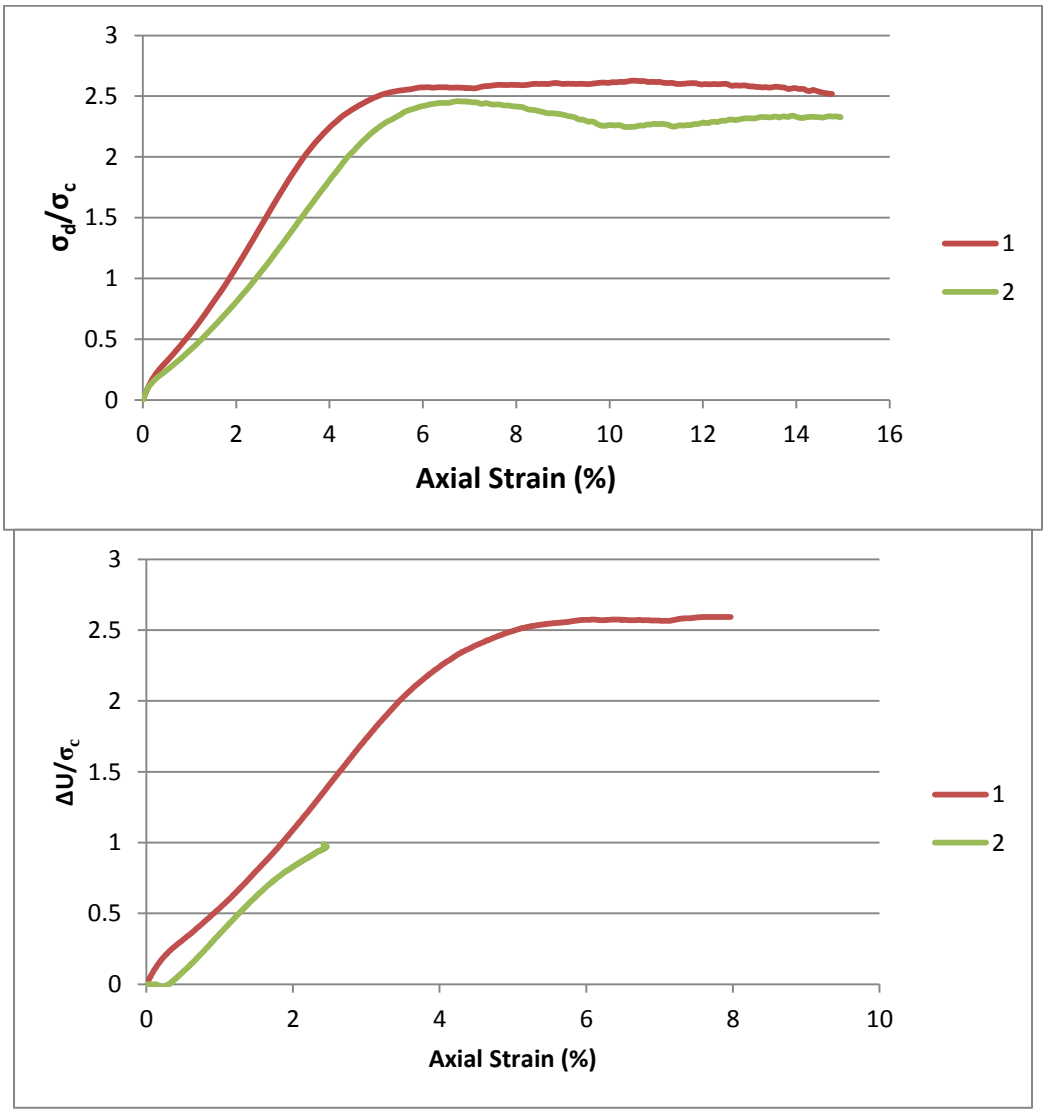

FIG 4.1. Ottawa 20-30 sand undrained triaxial compression loading test results for a relative density of 60% at an isotropic confining pressure of 60 kPa.

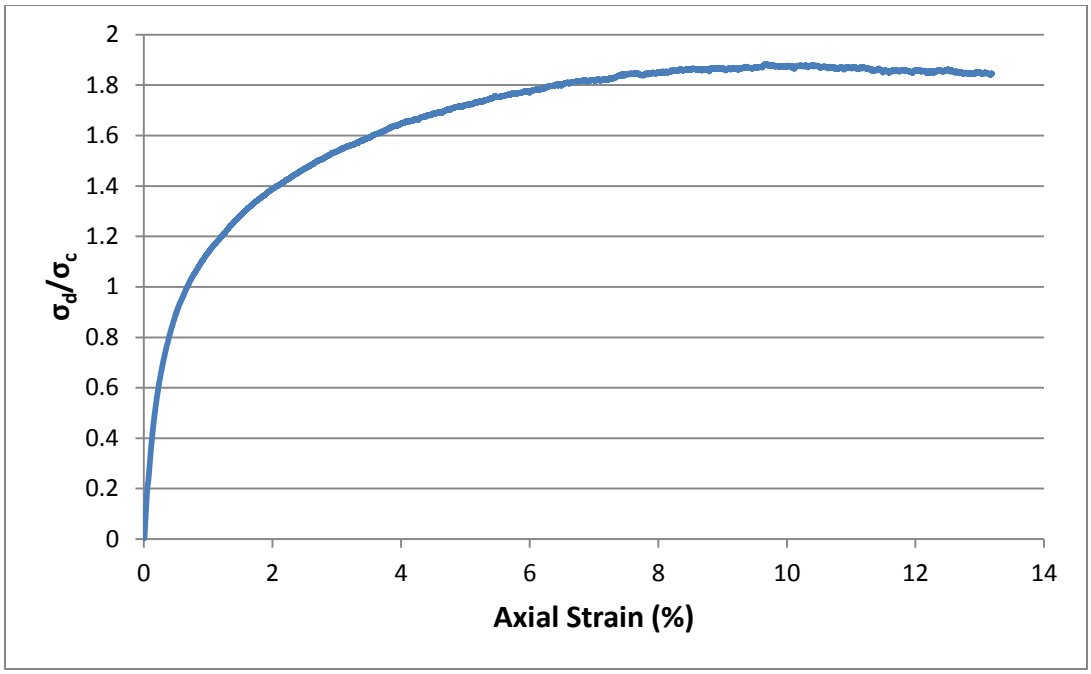

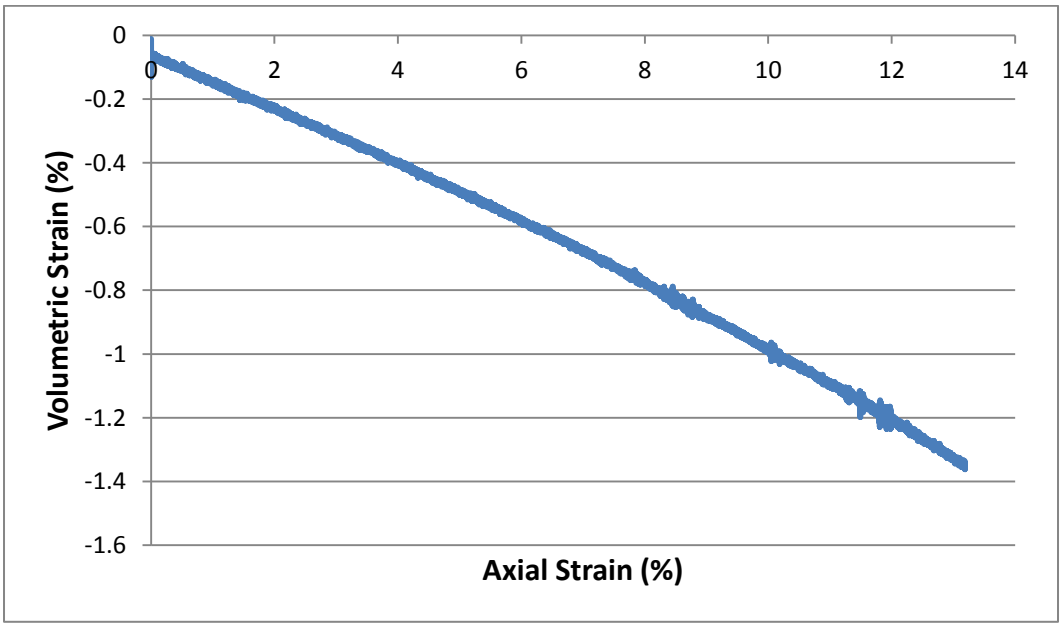

FIG 4.2. Ottawa 20-30 sand drained triaxial compression loading test results for a relative density of 36% at an isotropic confining pressure of 100 kPa.

4.1.2 Ottawa F60

Ottawa F60 sand was placed into the centrifuge model box using the air pluviation method developed by Katapa (2011). The lowest achievable relative density when pluviating the sand into the model box was 53%. The shear strength of the Ottawa F60 Silica sand was determined by triaxial testing. Ottawa F60 sand was air-pluviated at a relative density of 53% into a split mold lined with a membrane and mounted on the base of the triaxial cell. Figure 4.3 shows the results of two undrained triaxial compression tests conducted on Ottawa F60 sand at a relative density of 53% at a confining pressure of 60 kPa.

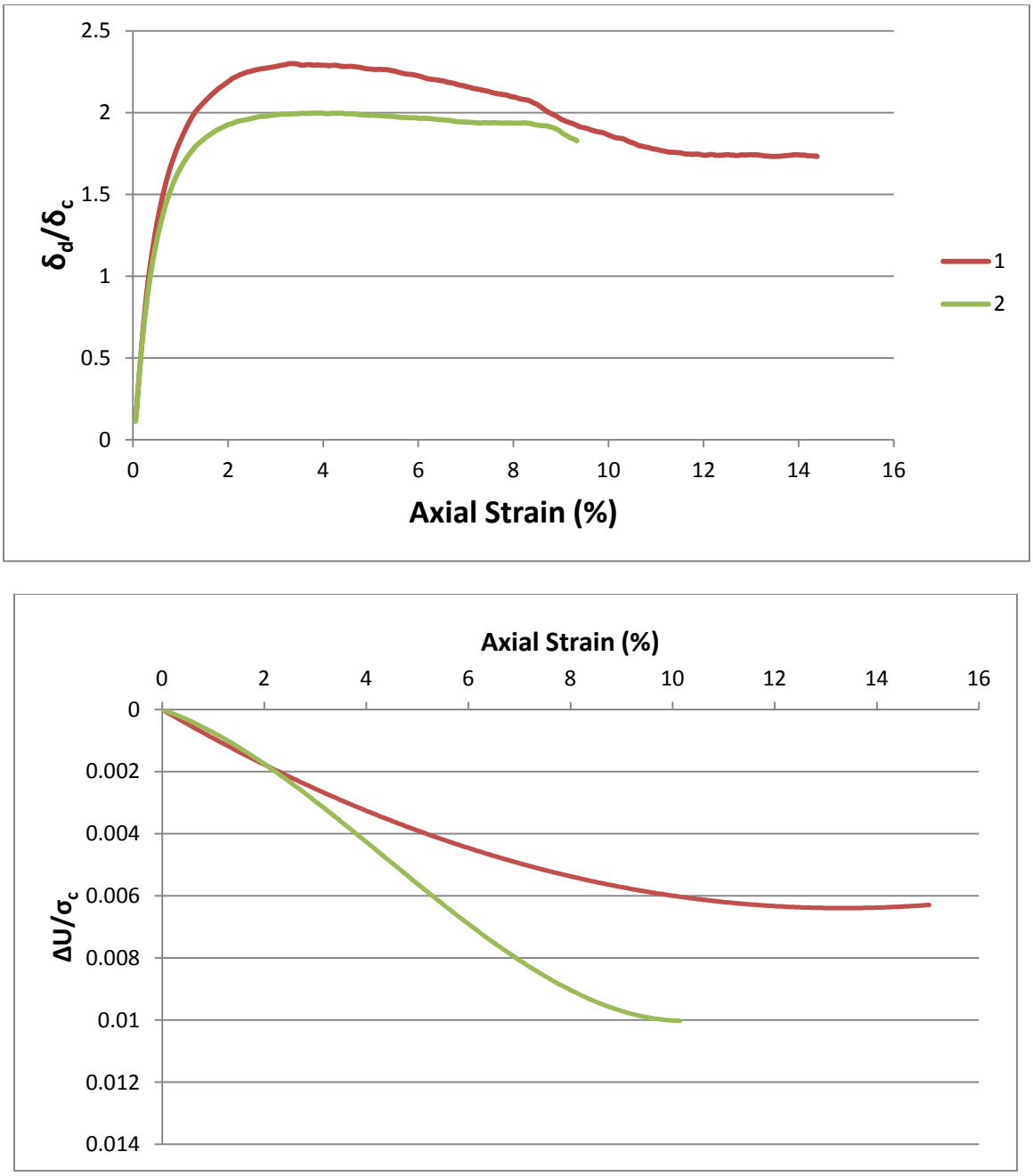

FIG. 4.3. Ottawa F60 undrained triaxial compression loading test results for a relative density of 53% at an isotropic confining pressure of 60 kPa.

4.2 Centrifuge Testing

4.2.1 Initial Ottawa 20-30 Tests

Two visits were made to UC Davis in an attempt to liquefy Ottawa 20-30 sand in the Schaevitz centrifuge. The first visit was made in the summer of 2011. The first set of three tests, on models designated C1-1, C1-2, and C1-3, consisted of Ottawa 20-30 sand air-pluviated with a drop height of 21 mm from the bottom screen which resulted a relative density of 60%. All three tests used water as pore fluid and employed the rigid model box. Table 4.1 summarizes the test parameters for the first three tests. These three tests were conducted using a centrifuge acceleration of 30 g and an earthquake motion modeled after the 1960 Chile earthquake with a prototype horizontal acceleration of 0.30 g. All of these three tests were deemed unsuccessful in that there was no evidence of liquefaction. The lack of evidence of liquefaction was initially attributed to either inadequate saturation or the use of the rigid box.

The second visit to UC Davis to tests Ottawa 20-30 sand was made during the winter of 2011. Two tests, on models designated C2-1 and C2-2, were conducted during this visit, one in the rigid box and one in the laminar box. These tests were also conducted using a centrifuge acceleration of 30 g and the Chile earthquake motion with a prototype horizontal acceleration of 0.30 g. Both tests employed Ottawa 20-30 sand air-pluviated into the model box at a relative density of 58%. Again, both tests were deemed unsuccessful due to the absence of any evidence of liquefaction. In diagnosing these test results, it was ultimately concluded that the problem was that the pore pressure dissipated too rapidly in the Ottawa 20-30 sand, i.e. that pore pressure dissipation during shaking prevented the soil from liquefying. One way to look at this problem is to consider that,

because of centrifuge scaling, the Ottawa sand particles simulated like a one inch-diameter clean gravel at field scale. Table 4.1 summarizes Ottawa 20-30 sand centrifuge tests conducted at UC Davis.

Table 4.1 Summary of Ottawa 20-30 sand centrifuge tests.

Test #	Date	Relative Density	Container	Motion	Centrifuge g Level	PGA (g)	Comments
C1-1	Jul-11	60%	Rigid	Chile	30	0.3	No liquefaction observed
C1-2	Jul-11	60%	Rigid	Chile	30	0.3	No liquefaction observed
C1-3	Jul-11	60%	Rigid	Chile	30	0.3	No liquefaction observed
C2-1	Dec-11	58%	Rigid	Chile	30	0.3	No liquefaction observed
C2-2	Dec-11	58%	Laminar	Chile	30	0.3	No liquefaction observed

4.2.2 Ottawa F60 Tests

Two options were considered to address the problems encountered when attempting to liquefy Ottawa 20-30 sand in the centrifuge: using a more viscous pore fluid or using a less permeable soil. The decision was made to use a less permeable soil, Ottawa F60 sand, as there was concern that the more viscous pore fluid would unrealistically affect the resedimentation of the soil after liquefaction. Two additional trips were taken to the UC Davis centrifuge facility to induce liquefaction conduct tests using the F60 sand.

The set of tests conducted using the F60 sand employed three different models being built at a relative density of 53%, designated models C3-1, C3-2, and C3-3. The first model, model C3-1, was spun up to a centrifuge acceleration of 30 g and shaken

twice. The first motion was a 50 Hz sine wave. The second motion was again a motion intended to simulate 1960 Chile earthquake with a prototype horizontal peak ground acceleration of 0.30 g. The model showed minimal settlement when subject to the first motion. When subject to the second motion, substantial settlement occurred in the model. Furthermore, bubbles could be seen coming up to the surface of the soil by the end of the test. The settlement of the soil was almost instantaneous, while the bubbles started coming up in the middle of the model during the motion and along the sides and wall of the model when the motion was stopped.

The second model built for the third set of tests on the UC Davis centrifuge, model C3-2, had a geomembrane placed on the surface of the soil to simulate a soil confining layer. The model was subjected to three different motions at a centrifuge acceleration of 30 g. The first two motions were sine waves. The first had a frequency of 50 Hz. Due to problems with instrumentation, the exact value of the second sine wave frequency was not determined. The last model was the strongest motion available at the time of testing. However, this shake was an earthquake-like motion smaller than the 1960 Chile earthquake motion usually used. The motion intended to simulate the 1960 Chile earthquake was not used because of equipment problems. When subject to the third motion, the soil settled, some bubbles were seen along the sides of the membrane, and a relatively large bulge (a bulge approximately 1.5 in. diameter) was visible in the membrane. Also, a significant depth of water was accumulated above the geomembrane.

The third model built for the third sequence of centrifuge tests model C3-3, differed substantially from the other two models in this test series. Sand was pluviated up to a height of 6 in. Then a steel plate with a height of 1.5 in. and a length of 4.5 in. was

placed on the soil surface at one side of the model to simulate an embankment load. The simulated embankment had a total weight of 15 pounds. Colored sand columns were placed in the model to facilitate detection of any failure plane that might develop within the soil model. After the motion was triggered and the embankment settled into the model a little more than ½", sand columns showed a clear failure plane within the soil. Figure 4.4 shows the displaced vertical soil columns in the soil grade.

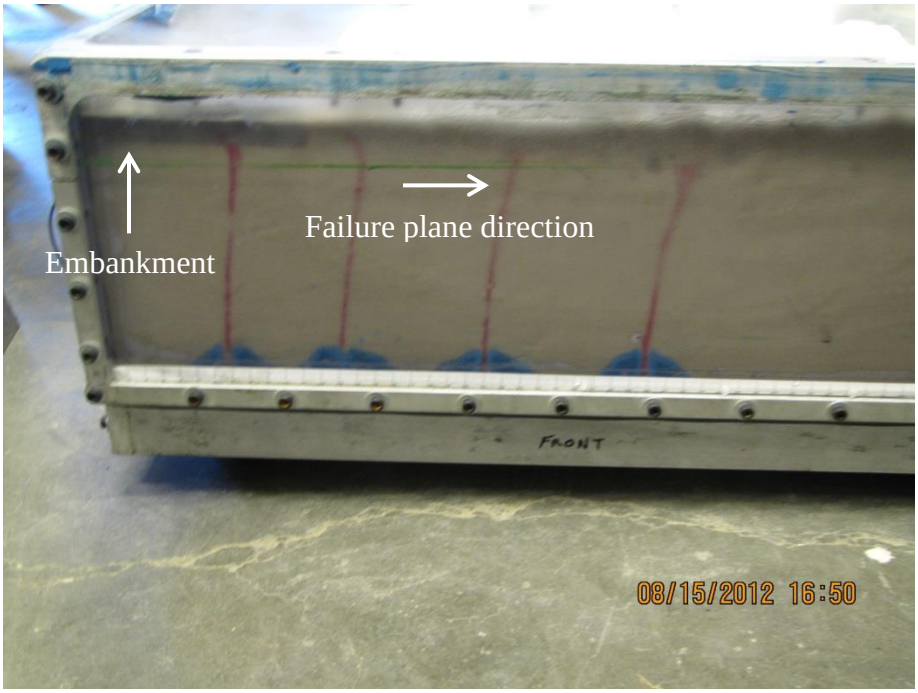

FIG 4.4. Failure plane for Model C3-3 embankment test.

During the last (fourth) trip to UC Davis, three additional centrifuge tests were conducted using Ottawa F60 sand. These tests in this fourth series were designated C4-1, C4-2, and C4-3. All three tests were conducted at a centrifuge acceleration of 30 g. The first test, on the model designated C4-1, was the same as the embankment test conducted in the previous visit except that a number of horizontal colored sand layers were added to

provide evidence of any sand boils that developed during or after the test. The second test, on the model designated C4-2, was a simple Ottawa F60 sand model. It was shaken with the 1960 Chile earthquake motion which had a prototype horizontal acceleration of 0.3 g. This test showed some bubbles and about ½ in. of settlement in the model. The third test, on the model designated C4-3, was the essentially same as the geomembrane test from the previous visit. However, this time a layer of sand was added to the top of the geomembrane and colored sand layers were placed in the model to provide visual evidence of sand boils. This proved to be of no help since only settlement was visible in the model. Table 4.2 summarizes Ottawa F60 sand centrifuge tests conducted at UC Davis.

Table 4.2. Summary of Ottawa F60 sand centrifuge tests.

Test #	Date	Relative Density	Container	Motion	G level	PGA	Comments
C3-1	May-12	53%	Rigid	Sine 50 Hz ,Chile	30	0.3	bubbling, settlement
C3-2	May-12	53%	Rigid	Sine 50 Hz, Sine	30	NA	geomembrane, bubbling, settlement
C3-3	May-12	53%	Rigid	Chile	30	0.3	embankment, failure plane present
C4-1	Aug-12	53%	Rigid	Chile	30	0.3	embankment, failure plane present
C4-2	Aug-12	53%	Rigid	Chile	30	0.3	bubbling, 1/2" settlement
C4-3	Aug-12	53%	Rigid	Chile	30	0.3	settlement

4.2.3 Instrumentation

As noted in Section 3.3.1, pore pressure transducers accelerometers, and an LVDT were also included in most of the tests conducted at UC Davis. Table 4.3 shows the specifics of instrumentation for each of the centrifuge tests conducted at UC Davis.

This data has been uploaded to the data library of the Network for Earthquake Engineering Simulation Research (NEESR). However, as noted previously the pore pressure data is considered unreliable.

Table 4.3. Instrumentation for UC Davis centrifuge tests.

Test #	Date	Container	Soil Type	Accelerometers	Pore Pressure Transducers	LVDT	Video
C1-1	Jul-11	Rigid	20-30	3	3	1	NO
C1-2	Jul-11	Rigid	20-30	3	3	1	NO
C1-3	Jul-11	Rigid	20-30	3	3	1	NO
C2-1	Dec-11	Rigid	20-30	4	3	1	NO
C2-2	Dec-11	Laminar	20-30	3	1	1	NO
C3-1	May-12	Rigid	F60	4	2	1	NO
C3-2	May-12	Rigid	F60	4	2	1	NO
C3-3	May-12	Rigid	F60	0	0	1	NO
C4-1	Aug-12	Rigid	F60	3	0	1	NO
C4-2	Aug-12	Rigid	F60	2	0	1	YES
C4-3	Aug-12	Rigid	F60	1	0	1	YES

4.3 Shake Table Testing

Shake table tests on Ottawa 20-30 Crystal Silica sand were conducted at ASU. These tests were conducted to induce liquefaction on Ottawa 20-30 Crystal Silica sand since liquefaction was not achieved at UC Davis. Evaluation of the effect of liquefaction on the microstructure of Ottawa 20-30 Crystal Silica sand was considered particularly important, as this material is widely used in geotechnical studies and may be considered a standard test sand.

The model for the shake table test at ASU conducted using Ottawa 20-30 Crystal Silica sand was designated S1-1. The test soil was placed in the model box using the

sedimentation process. The relative density that was achieved by this method was 36%. A colored sand layer was placed about ¾ from the bottom of the box to observe liquefaction phenomena. The model box was then shaken for about 10 seconds using the 10 Hz sine wave with a displacement of .75 mm (resulting in a peak ground acceleration of 0.3 g). The Ottawa 20-30 Crystal Silica sand settled about an inch throughout the model. The colored sand remained horizontal but some colored sand particles did bubble to the surface. Table 4.4 summarizes the ASU shake table test.

Table 4.4. Summary of ASU shake table test (Ottawa 20-30 sand).

Test #	Date	Relative Density	Container	Motion	G level	PGA	Comments
S1-1	June-13	36%	Rigid	Sine 10 Hz .75 mm disp.	NA	0.3	bubbling, settlement

4.4 Core Specimens

Core specimens with a diameter of 1.4" were acquired from every test run at UC Davis and ASU. The core specimens were obtained using the method developed by Katapa (2011). Selected specimens were stabilized using the procedure developed by Czupak (2011). Table 4.5 summarizes the core specimen details.

Table 4.5. Core specimen details.

Specimen	Test #	disposition of core	Location	Notes
BO1	NA	stabilized,CT scanned	center of box	baseline Ottawa 20-30 specimen
BF1	NA	stabilized, CT scanned	center of box	baseline F60 specimen
C-1-1-1	C1-1	not used	NA	no liquefaction
C-1-1-2	C1-1	not used	NA	no liquefaction
C-1-1-3	C1-1	not used	NA	no liquefaction
C-1-1-4	C1-1	not used	NA	no liquefaction
C-1-2-1	C1-2	not used	NA	no liquefaction
C-1-2-2	C1-2	not used	NA	no liquefaction
C-1-2-3	C1-2	not used	NA	no liquefaction
C-1-3-1	C1-3	not used	NA	no liquefaction
C-1-3-2	C1-3	not used	NA	no liquefaction
C-2-1-1	C2-1	not used	center, close to wall	no liquefaction
C-2-1-2	C2-1	not used	center, close to wall	no liquefaction
C-2-2-1	C2-2	not used	8" from side, center	no liquefaction
C-2-2-2	C2-2	not used	8" from side, center	no liquefaction
C-2-2-3	C2-2	not used	center of box	no liquefaction
C-3-1-1	C3-1	stabilized	center, close to wall	on possible sand boil
C-3-1-2	C3-1	stabilized	7" from side,center, close to wall	on possible sand boil
C-3-1-3	C3-1	not used	6" from side, center, opposite wall	on possible sand boil
C-3-2-1	C3-2	not used	center, 2" from wall	on bulge observed
C-3-3-1	C3-3	stabilzed, CT scanned	1" from embankment	failure plane present
C-3-3-2	C3-3	not used	center, close to wall	possible failure plane

C-4-1-1	C4-1	stabilized, CT scanned	1" from embankment	failure plane present
C-4-1-2	C4-1	stabilized, CT scanned	1" from embankment	failure plane present
C-4-1-3	C4-1	not used	center, close to wall	possible failure plane
C-4-1-4	C4-1	not used	center, close to wall	possible failure plane
C-4-1-5	C4-1	not used	2" from embankment	possible failure plane
C-4-1-6	C4-1	not used	2" from embankment	possible failure plane
C-4-2-1	C4-2	stabilized	center of box	liquefied soil
C-4-2-2	C4-2	stabilized	center of box	liquefied soil
C-4-2-3	C4-2	not used	6" from side, center	liquefied soil
C-4-2-4	C4-2	not used	6" from side, center	liquefied soil
C-4-2-5	C4-2	not used	6" from side, center	liquefied soil
C-4-2-6	C4-2	not used	6" from side, center	liquefied soil
C-4-3-1	C4-3	not used	center	could not core completely
S-1-1-1	S1-1	stabilized, CT scanned	center	possible sand boil
S-1-1-2	S1-1	not used	center	liquefied soil

Chapter 5

5 CT SCANS AND IMAGE ANALYSIS

5.1 Introduction

This section covers the results of CT scan image processing of the specimens selected for analysis of local void ratio distribution for the purpose of this study. The results that were analyzed for the purpose of this study were:

- CT scans of Czupak's (2011) Ottawa 20-30 specimen (for comparison with the results of optical image analysis conducted by Czupak (2011)
- CT scans of liquefied Ottawa 20-30 sand specimens from ASU shake table test (test designation S1-1)

The Ottawa F60 CT scan images were not analyzed because the resolution was too low to provide information on a particle-sized scale.

5.2 Comparison of CT Scan and Optical Imaging Results

The Ottawa 20-30 sand specimen that Czupak (2011) analyzed with optical microscopy was sent for CT scan imaging to UT Austin. The CT scan was analyzed using Avizo® Fire and the procedure covered in a previous section of this dissertation (Section 3.5.1). CT scan images were analyzed for local void ratio using different subvolumes sizes and a total of 13 slices which amounted to a thickness of 0.0464 mm. These subvolumes were the total sample size (~24,000 microns) and sub-volumes of 16000 x 16000 microns, 16000 x 8000 microns, 8000 x 8000 microns, and 4000 x 4000 microns. These subvolume sizes were chosen to coincide with the volume sizes analyzed by Czupak (2011). The first step taken to compare the two methods was to calculate the

mean void ratio values for the CT scan images and compare them to the mean void ratio values established by Czupak (2011). Table 5.1 shows the resulting comparison.

Table 5.1. Mean Void Ratio for CT and BFM for Different Subvolumes.

Subvolume Size (μm)	BFM Mean Void Ratio (Control Sample)	CT Scan Mean Void Ratio
D = 23,649	0.5475	-
16000 x 16000	0.5491	0.7678
16000 x 8000	0.5513	0.7993
8000 x 8000	0.5429	0.5743
4000 x 4000	0.4561	0.5486

A total volume mean void ratio was not calculated for CT scan images due to limitations of the software. In Avizo Fire, subvolumes have to be rectangular. For comparison with results from Czupak (2011), a cubical volume was used and the largest cube that could be inscribed within the specimen was 16000 μm in dimension.

From the comparison of mean void ratios, it was determined that the use of subvolumes larger than 4000 x 4000 microns within Avizo Fire was not satisfactory for proper image analysis. This was due to limitations of the threshold quantification tool. For larger subvolumes, it was extremely difficult to obtain the correct threshold window. This difficulty led to erroneous void ratio calculations for larger subvolumes, as seen from the data in Table 5.1. Note, however, that the optical method lost accuracy when the area was than 8000 x 8000 microns. Thus, the CT scan results for a 4000 x 4000 micron subvolume was compared to optical results for an 8000 x 8000 micron area for the comparison between the two methods (optical image (or BFM) analysis and CT scan analysis). These frequency diagrams are presented in Figure 5.1.

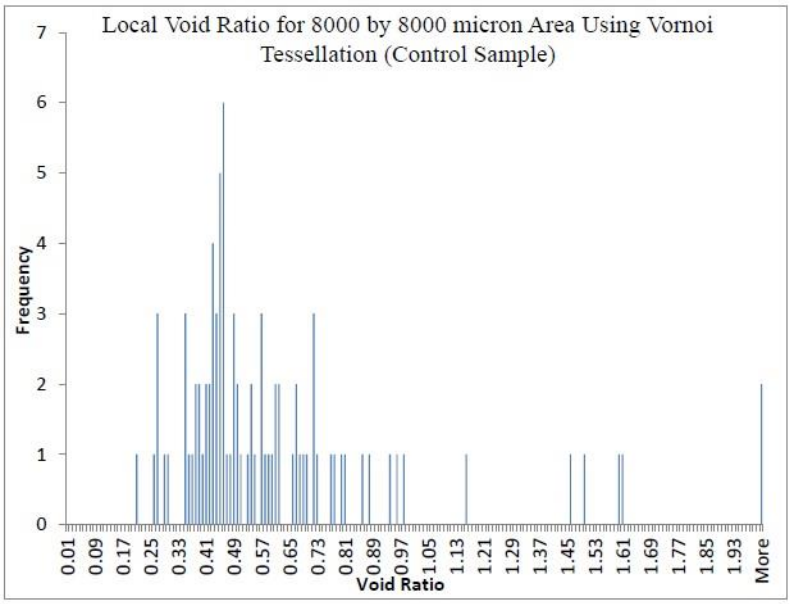

(a)

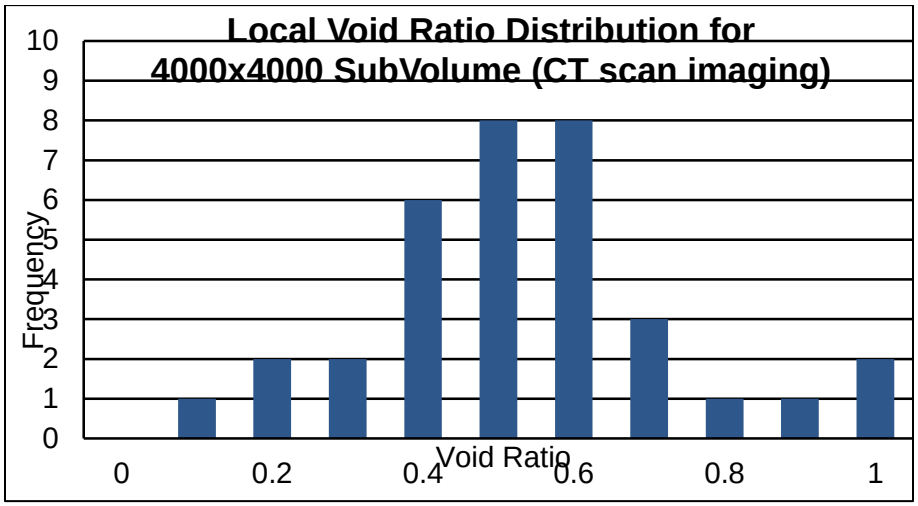

(b)

FIG. 5.1. Local void ratio distribution for (a) 8000 x 8000 microns for BFM (Czupak, 2011) and (b) 4000 x 4000 microns for CT.

The standard deviation for each of the subvolumes using CT scan imaging was calculated. Figure 5.2 shows the standard deviation from the mean void ratio vs. the subvolume size.

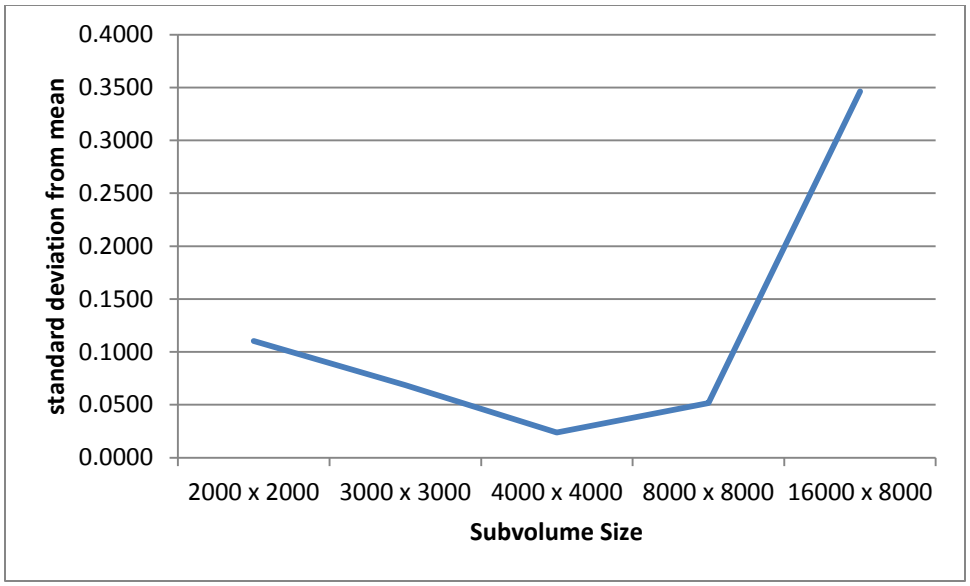

FIG. 5.2. Standard deviation vs. subvolume size of CT scan images.

The similarity of the void ratio distribution histogram and of the mean void ratio (0.5486) calculated using CT scans for a 4000 x 4000 micron subvolume to the void ratio histrogram and the mean void ratio (0.5475) using an 8000 x 8000 micron area analyzed by Czupak (2011) along with the smaller standard deviation for the CT scan data led to the conclusion that the use of CT scan imaging for local void ratio distribution using a 4000 micron by 4000 micron subvolume is satisfactory.

5.3 Impact of Liquefaction on Ottawa 20-30 Sand Specimens

The mean void ratio and standard deviation were calculated for both the baseline Ottawa 20-30 sand specimen created by sedimentation (BO1) and the liquefied Ottawa 20-30 sand specimen from the ASU shake table test (S1-1-1). Figure 5.3 shows the resulting mean void ratio and standard deviation vs. subvolume size plots acquired from the image analysis procedure for the baseline Ottawa 20-30 sand specimen (BO1).

Figure 5.4 shows the resulting mean void ratio and standard deviation vs. subvolume size plots acquired from the image analysis procedure for the liquefied Ottawa 20-30 sand specimen (S1-1-1).

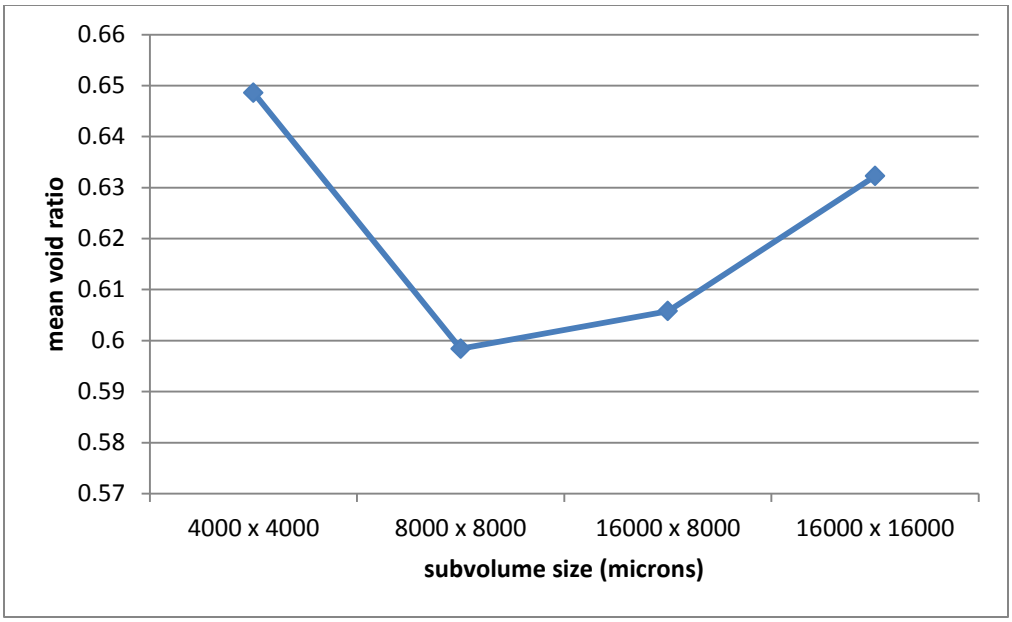

(a)

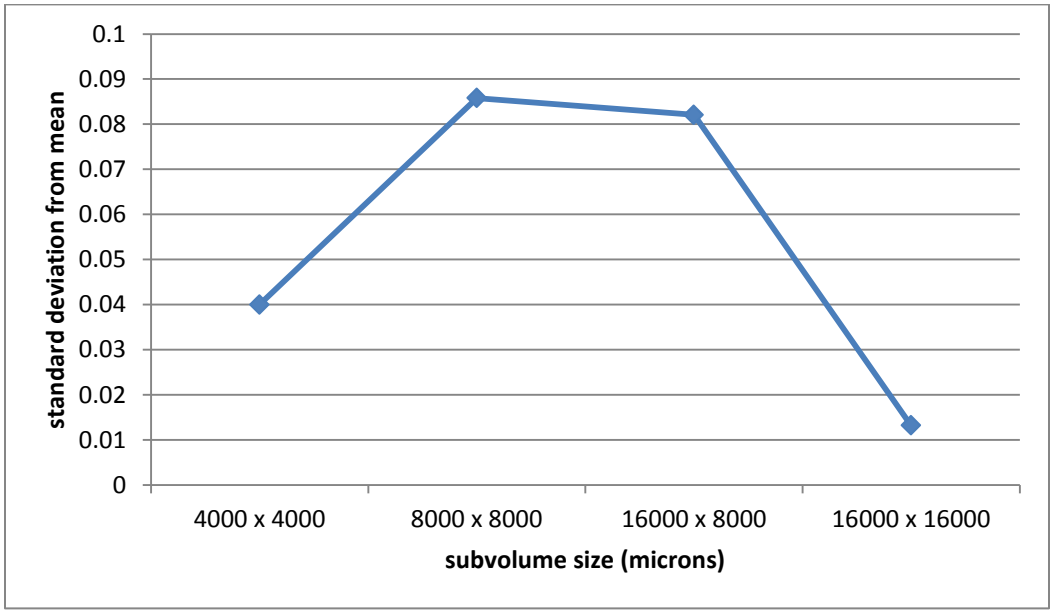

(b)

FIG. 5.3. (a) Mean void ratio vs. subvolume size and (b) standard deviation vs. subvolume size for baseline Ottawa 20-30 sand specimen (BO1).

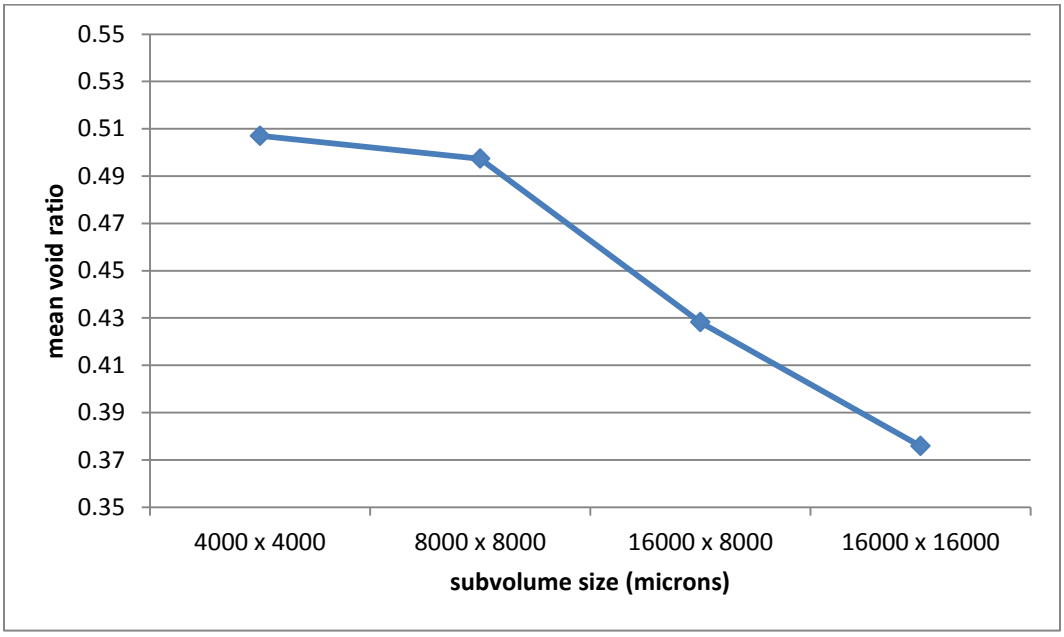

(a)

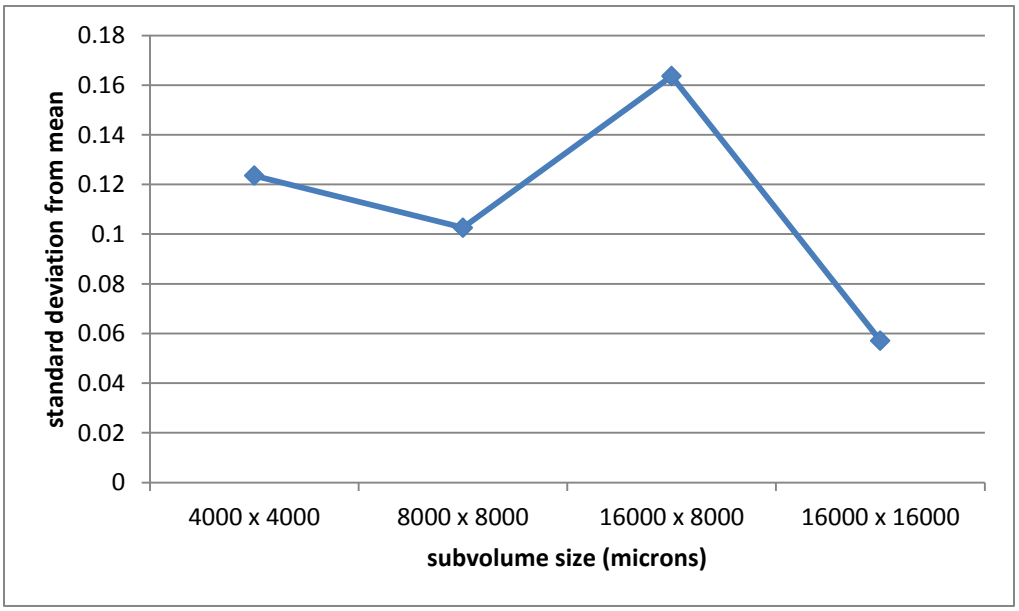

(b)

FIG. 5.4. (a) Mean void ratio vs. subvolume size and (b) standard deviation vs. subvolume size for liquefied Ottawa 20-30 sand specimen (S1-1-1).

Figure 5.3 shows that the mean void ratio ranged between 0.59 and 0.65 for the different subvolume sizes for the baseline specimen (i.e. prior to liquefaction). This mean void ratio range is equivalent to a relative density range of 38% to 63%. This level of variability in local void ratio was expected since relative densities calculated for 1.4 inch-diameter specimens of Ottawa 20-30 sand created by sedimentation within the model box and recovered without being subject to liquefaction had a similar range in relative density. Despite the range in local void ratio, Figure 5.3 also suggest that the model was relatively homogenous as the standard deviation was less than 0.1 for all subvolume sizes. Again, the 4000 x 4000 micron subvolume proved to be the most representative for analysis due to its proximity to the calculated mean void ratio and its low standard deviation from the mean.

Figure 5.4 shows that the mean void ratio ranges between 0.51 and 0.375 for the different subvolume sizes for the post-liquefaction specimen. This mean void ratio range is equivalent to a relative density range of 97% to above 100%. This was expected, as the soil was observed to have densified (settled) after liquefaction. However, the standard deviation of the post-liquefaction specimen was significantly higher than of the baseline specimen, with the values for the subvolumes less than 16000 x 16000 microns all greater than 0.1. This was expected as, even though the soil model densified overall, some pockets of loose soil (i.e. high void ratio) were observed during image processing. These soil pockets were along the rim of a possible sand boil that went through the middle of the specimen. Figure 5.5 shows the frequency histogram for the local void ratio of the liquefied specimen. Figure 5.5 shows the specimen relatively high frequency of high void ratio (void ratio greater than 0.6) subvolumes, suggesting zones of loosened soil in the

sand boil that was captured along the edge of the specimen due to upward flow of pore water following liquefaction.

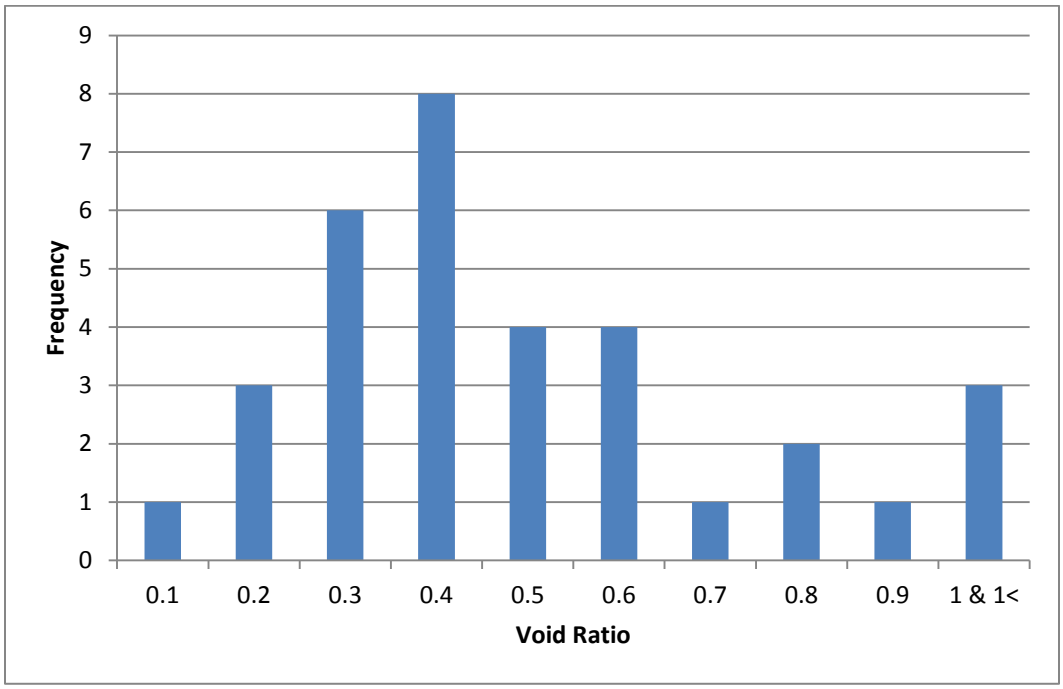

FIG. 5.5. Frequency histogram of local void ratio in liquefied specimen.

5.4 CT Scans for Ottawa F60 Sand Specimens

The baseline sample of Ottawa F60 sand (BF1) was sent for CT scans to UT Austin along with 3 failure plane specimens of F60 sand (C3-3-1, C4-1-1, C4-1-2). Unfortunately, the resolution of the CT scan imaging was not satisfactory for image analysis. Therefore, no analysis was completed on the Ottawa F60 sand specimens.

Chapter 6

6 SUMMARY AND CONCLUSIONS

6.1 Summary

The objective of this study was to evaluate the changes in the microstructure of a cohesionless soil due to seismically induced liquefaction. This study consisted of creating liquefiable soil deposits, inducing liquefaction in the deposits, acquiring samples, imaging the samples, and determining the local void ratio distribution in the sand specimens using image analysis. As part of this study, the use of CT scan images as a reliable imaging method for void ratio analysis was also investigated. The liquefiable soil deposits were created by air-pluviation and sedimentation. The soil deposits were then liquefied at the UC Davis centrifuge facility and on a shake table at ASU. Initial tests at UC Davis employed Ottawa 20-30 sand. However, the Ottawa 20-30 sand proved to be too permeable to liquefy in the centrifuge. Therefore, Ottawa F60 sand was employed on the centrifuge testing program. The ASU shake table tests employed Ottawa 20-30 sand.

The soil in the models was frozen and cores of non-liquefied and liquefied soil were obtained using the method developed by Katapa (2011). The recovered cores were then stabilized with optical grade epoxy using the method developed by Czupak (2011). Selected stabilized cores were then sent for CT scan imaging to UT Austin. A comparison between optical imaging and CT scan imaging of an Ottawa 20-30 sand core was done to establish CT imaging as a reliable method. Then, a comparison of baseline and liquefied Ottawa 20-30 sand specimens was completed to investigate changes in the

soil microstructure due to liquefaction. A comparison between baseline and liquefied Ottawa F60 sand specimens was attempted but the CT scan images for F60 sand did not have the required resolution to make this comparison.

6.2 Conclusions

In this study, a method for analyzing CT scan images to investigate the local void ratio distribution in sand specimens was developed. In the first part of the research, the results with respect to local void ratio distribution from the CT scan processing were compared to results from analysis of optical images. The conclusions from this part of the study were:

- Thresholding is the most important part of the CT scan analysis procedure
- The use of a 4000 x 4000 micron subvolume for CT scan image analysis was determined as the best subvolume size for analysis of Ottawa 20-30 sand specimens as it gave the closest void ratio to the calculated void ratio and had a relatively low standard deviation;
- Using too large subvolume in the CT scan analysis causes errors that are likely due to inaccuracies associated with thresholding
- CT scan imaging can give similar results to optical imaging for local void ratio distribution of Ottawa 20-30 sand if the appropriate procedures are employed

The comparison between non-liquefied and liquefied Ottawa 20-30 sand specimens created by sedimentation resulted in the following conclusions:

- Post liquefaction densification of a soil deposit can result in low void ratios and correspondingly high relative densities;

- The liquefied soil was non-homogenous compared to the baseline soil specimen, possibly due to the inclusion of parts of a sand boil within the liquefied specimen.

6.3 Recommendations for Future Work

Recommendations for future work within this research study are as follows:

- True three-dimensional subvolumes (4000 x 4000 x 4000 micron) should be analyzed for local void ratio. Because only a limited number of slices were included in the analysis described herein, the volume analyzed in Avizo® Fire still represented essentially a two-dimensional slice through the specimen;
- An image analysis procedure that would analyze the particle orientation within the soil specimen should be developed and applied to the CT scans to see if liquefaction and the method of sample preparation (e.g. sedimentation versus pluviation) affect particle orientation;
- A more thorough analysis of the image analysis results should be conducted, including an analysis to try to isolate the sand boil zone within the liquefied core to determine if conclusions concerning loosening of the soil within the sand boil has occurred;
- The reasons for the poor resolution of the CT scans of the F60 sand specimens should be investigated to see if that situation can be remedied.

REFERENCES

Al-Raoush, R., and Alshibli, K.A. (2006) "Distribution of local void ratio in porous media systems from 3D x-ray micro-tomography images." *Physica A: Statistical Mechanics and its Applications*, Vol. 361 (March), No. 2, pp. 441-456.

Arulanandan, K. and Scott, R. (1993). "Project VELACS—Control Test Results." *J. Geotech. Engrg,*. 119(8), 1276-1292. Technical Papers

ASTM. (2006). "Standard test method for minimum index density and unit weight of soils and calculation of relative density D4254." *American Society of Testing and Materials*, West Conshohoken, PA.

ASTM. (2007). "Standard test method for particle-size analysis of soils D422." *American Society of Testing and Materials,* West Conshohoken, PA.

Batiste, S.N., Alshibli, K.A., Sture, S., and Lankton, M. (2004). "Shear band characterization of triaxial sand specimens using computed tomography." *Geotech. Testing J*., 27(6): 1-13.

Borja, R. I., Kavazanjian, E., & Evans, J. C. (2008). *Properties of Cohesionless Soil Subsequent Liquefaction and Resedimentation.* Proposal.

Czupak, Z. D. (2011). "Stabilization and Imaging of Cohesionless Soil Samples". *MS Thesis*, Arizona State University, Tempe, Arizona.

Dobry, R., Taboada, V., and Liu, L., (1995), "Centrifuge Modeling of Liquefaction Effects During Earthquakes*," Keynote Lecture, Proc., 1st Int'l Conf. on Earthquake Geotechnical Engineering*, Tokyo, Japan, Nov. 14-16, Reprint Vol., pp. 129-162.

Epotech (2009). "Removing bubbles from epoxy. Tech Tip 4." <http://www.epotek.com/SSCDocs/techtips/Tech%20Tip%204%20-%20Removing%20Bubbles.pdf>

Fiegel, G. L., Hudson, M., Idriss, I. M., Kutter, L. B., & Zeng, X. (1994). Effect of model containers on dynamic soil response. In Leung, Lee, & Tan (Ed.), *Centrifuge 94* (pp. 145-150). Rotterdam: Balkema.

Frost, J. D. (1989). "Studies on the Monotonic and Cyclic Behavior of Sand." *PhD Dissertation*, Purdue University, West Lafayatte, Indiana.

Frost, J.D., and Kuo, C.Y. (1996). "Automated determination of the distribution of local void ratio from digital images." *Geotech. Testing J.*, 19(2), 107-117.

Katapa, K. (2011). "Undisturbed sampling of cohesionless soils for evaluation of

mechanical properties and microstructure." *MS Thesis*, Arizona State University, Tempe, Arizona.

Kutter, B. L. (1992). "Dynamic Centrifuge Modeling of Geotechnical Structures", Transportation Research Record 1336, TRB, National Research Council, pp. 24-30, Washington, D.C.

Santamarina, C. J., & Cho, C. G. (2001, June). Determination of Critical State Parameters in Sandy Soils - Simple Procedure. *Geotechnical Testing Journal*, *24*(2), 185-192.

UC Davis (2013). "Schaevitz centrifuge image", Davis, CA. http://nees.ucdavis.edu/smallcentrifuge.php.

Ueno, K. (2000) "Methods for Preparation of Sand Samples". In Kusakabe, & Takemura (Ed.), *Centrifuge 98* (pp. 1047-1055). Tokyo: Balkema.

U.S. Silica Company (2011). "Product Data, ASTM 20/30 Underground Silica." Berkeley Springs, WV. <http://www.u-s-silica.com/media/12643/ottastm2030sand2000.pdf>

APPENDIX A

OTTAWA 20-30 SAND PRODUCT FACT SHEET

Product Data

US SILICA™

ASTM(1) 20/30

UNGROUND SILICA

PLANT: OTTAWA, ILLINOIS

(1) American Society for Testing and Materials

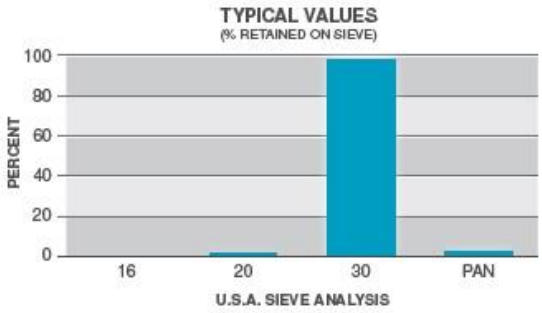

USA STD SIEVE SIZE		TYPICAL VALUES		
		% RETAINED		% PASSING
MESH	MILLIMETERS	INDIVIDUAL	CUMULATIVE	CUMULATIVE
16	1.180	0.0	0.0	100.0
20	0.850	1.0	1.0	99.0
30	0.600	97.0	98.0	2.0
Pan		2.0	100.0	0.0

TYPICAL PROPERTIES	
Color	White
Grain Shape	Round
Hardness (Mohs)	7
Melting Point (Degrees F)	3100
Mineral	Quartz
pH	7
Specific Gravity	2.65

CONFORMS TO ASTM C778

TYPICAL CHEMICAL ANALYSIS, %	
SiO_2 (Silicon Dioxide)	99.8
Fe_2O_3 (Iron Oxide)	0.020
Al_2O_3 (Aluminum Oxide)	0.06
TiO_2 (Titanium Dioxide)	0.01
CaO (Calcium Oxide)	<0.01
MgO (Magnesium Oxide)	<0.01
Na_2O (Sodium Oxide)	<0.01
K_2O (Potassium Oxide)	<0.01
LOI (Loss On Ignition)	0.1

December 15, 1997

U.S. Silica Company
8490 Progress Drive, Suite 300
Frederick, MD 21701
(301) 682-0600 (phone)
(800) 243-7500 (toll-free)
ussilica.com

WARNING: The product contains crystalline silica – quartz, which can cause silicosis (an occupational lung disease) and lung cancer. For detailed information on the potential health effect of crystalline silica - quartz, see the U.S. Silica Company Material Safety Data Sheet.

APPENDIX B

OTTAWA F60 SILICA SAND PRODUCT FACT SHEET

Product Data

US SILICA

F-60

UNGROUND SILICA

PLANT: OTTAWA, ILLINOIS

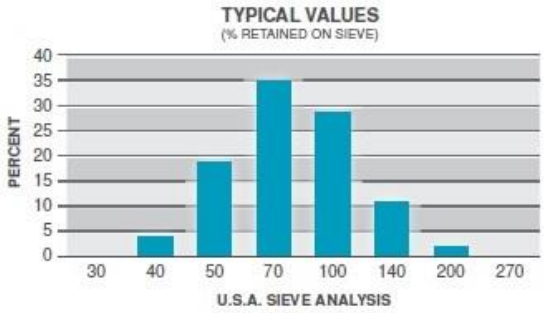

USA STD SIEVE SIZE		TYPICAL VALUES		
		% RETAINED		% PASSING
MESH	MILLIMETERS	INDIVIDUAL	CUMULATIVE	CUMULATIVE
30	0.600	0.0	0.0	100.0
40	0.425	4.0	4.0	96.0
50	0.300	19.0	23.0	77.0
70	0.212	35.0	58.0	42.0
100	0.150	29.0	87.0	13.0
140	0.106	11.0	98.0	2.0
200	0.075	2.0	100.0	0.0
270	0.053	0.0		

TYPICAL PHYSICAL PROPERTIES	
AFS(1) Acid Demand (@pH 7)	<1.0
AFS(1) Grain Fineness	60
Color	White
Grain Shape	Round
Hardness (Mohs)	7
Melting Point (Degrees F)	3100
Mineral	Quartz
Moisture Content (%)	<0.05
pH	7
Specific Gravity	2.65

(1) American Foundrymen's Society

TYPICAL CHEMICAL ANALYSIS, %	
SiO_2 (Silicon Dioxide)	99.8
Fe_2O_3 (Iron Oxide)	0.020
Al_2O_3 (Aluminum Oxide)	0.06
TiO_2 (Titanium Dioxide)	0.01
CaO (Calcium Oxide)	<0.01
MgO (Magnesium Oxide)	<0.01
Na_2O (Sodium Oxide)	<0.01
K_2O (Potassium Oxide)	<0.01
LOI (Loss On Ignition)	0.1

December 15, 1997

U.S. Silica Company
8490 Progress Drive, Suite 300
Frederick, MD 21701
(301) 682-0600 (phone)
(800) 243-7500 (toll-free)
ussilica.com